TR 91-01

THE PRECAMBRIAN IRON-FORMATIONS IN THE LIMPOPO BELT AS REPRESENTED BY THE MAGNETITE QUARTZITE DEPOSITS AT MOONLIGHT, KOEDOESRAND AREA, NORTHERN TRANSVAAL

BY

JACO CORNELIS BADENHORST

Submitted in partial fulfilment of the requirements for the degree of **MASTER OF SCIENCE - EXPLORATION GEOLOGY** in the faculty of Science, Rhodes University.

ABSTRACT

This dissertation is based largely on data that was accumulated during the execution of an exploration program by Iscor Ltd in the Northern Transvaal. The program included geological mapping, geophysical surveys and drilling, on Precambrian iron-formations in the Central Zone of the Limpopo Belt. The structure, stratigraphy, metamorphism, and economic importance of the magnetite quartzites and associated lithologies of the Moonlight prospect are discussed.

The lithologies underlying the Moonlight prospect area consist of various pink- and grey-banded gneisses and pink granulite, together with a variety of metasedimentary supracrustal rock-types and concordant serpentinite bodies. The gneissic rock-types consist of chlorite-quartz-feldspar gneiss, chlorite-quartz-feldspar augen gneiss, hornblende-quartz-feldspar gneiss, biotite-quartz-feldspar gneiss, felsic and mafic granulite, and foliated amphibolite. The metasedimentary lithologies are represented by calc-silicates and marble, white quartz-feldspar granulite, magnetite quartzite, metaquartzite and garnet-bearing granulite and gneiss (metapelites). The concordant ultramafic bodies consist of serpentinite with lesser amphibolite, dunite, and chromitite. Intrusive pegmatites and diabase dykes are also present in the prospect area.

Metamorphism reached granulite-facies, and more than one retrograde metamorphic event is recognized. Amphibolite-facies assemblages are present, but it is uncertain whether they represent another retrograde event. Polyphase deformation has produced intense and complex folding, resulting in irregular magnetite quartzite orebodies. The high metamorphic grades have resulted in medium-grained recrystallization of the magnetite-quartzites with a loss of prominent banding often associated with these rock-types.

The magnetite quartzite occurs as three seperate but related ore zones, consisting of one or more ore-bands seperated by other lithologies. All three zones form poor outcrops and suboutcrops in a generally flat lying and sand covered area. Although representing a low-grade iron ore (32 % total Fe), the magnetite quartzite deposits at Moonlight are regarded as potentially viable due to the large

opencast tonnages available at low stripping ratios, and the relatively cheap and easy beneficiation process needed to produce a magnetite concentrate with 69-70% total Fe.

PREFACE AND ACKNOWLEDGEMENTS

The description of certain aspects of the geology of the Precambrian rocks in the Koedoesrand Area is based on observations which have been made over a period of three years, during which the writer was engaged as a project geologist for Iscor Ltd. Free use has been made of draughting and laboratory facilities at Iscor Headquarters, Pretoria. Thanks are thus due to all Iscor personnel involved in the Moonlight project, especially Mr D C Page for many fruitfull discussions.

Special thanks to Prof. F Piranjo, Mr C Mallinson, and other members of the geological staff at Rhodes University, for constructive discussion and critisism, and for me being able to use all departemental facilities available.

This dissertation is dedicated to my wife and son for their unselfish affection and understanding throughout my study years.

CONTENTS

CONTENTS (continued) PAGE

LIST OF FIGURES PAGE

LIST OF FIGURES (continued)

LIST OF TABLES

PAGE

LIST OF PLATES

BACK POCKET

1. INTRODUCTION

1.1 STUDY AREA

An exploration project was conducted on the farm Moonlight 111LR, 1 421 hectares in extent and situated approximately 160 km north-west of Potgietersrust in an area, generally known as the Koedoesrand Area (fig 1).

The project-area is situated in the Central Zone of the Limpopo Belt and is thus underlain by a wide variety of high grade and complexly deformed rock-types. Although most of the work concentrated on the Moonlight project area (figures 3 and 4), additional work was conducted on a regional scale of which some information is included in this dissertation.

1.2 INFRASTRUCTURE

Moonlight is located on longitude 28°13' and latitude 22°30' and has an average elevation of 970m ams.

"Strategic" points in relation to the project area, are listed below:

Towns:	Pietersburg	180 km south-east
	Potgietersrust	175 km south-south-east
	Pretoria	350 km south
Escom power-station:	Ellisras (Matimba)	80 km south-west
Escom power-line:	Moonlight	on site
Tar roads:	Marnitz	10 km north
	Marken-Ellisras	30 km south
Railway line:	Ellisras	80 km south-west

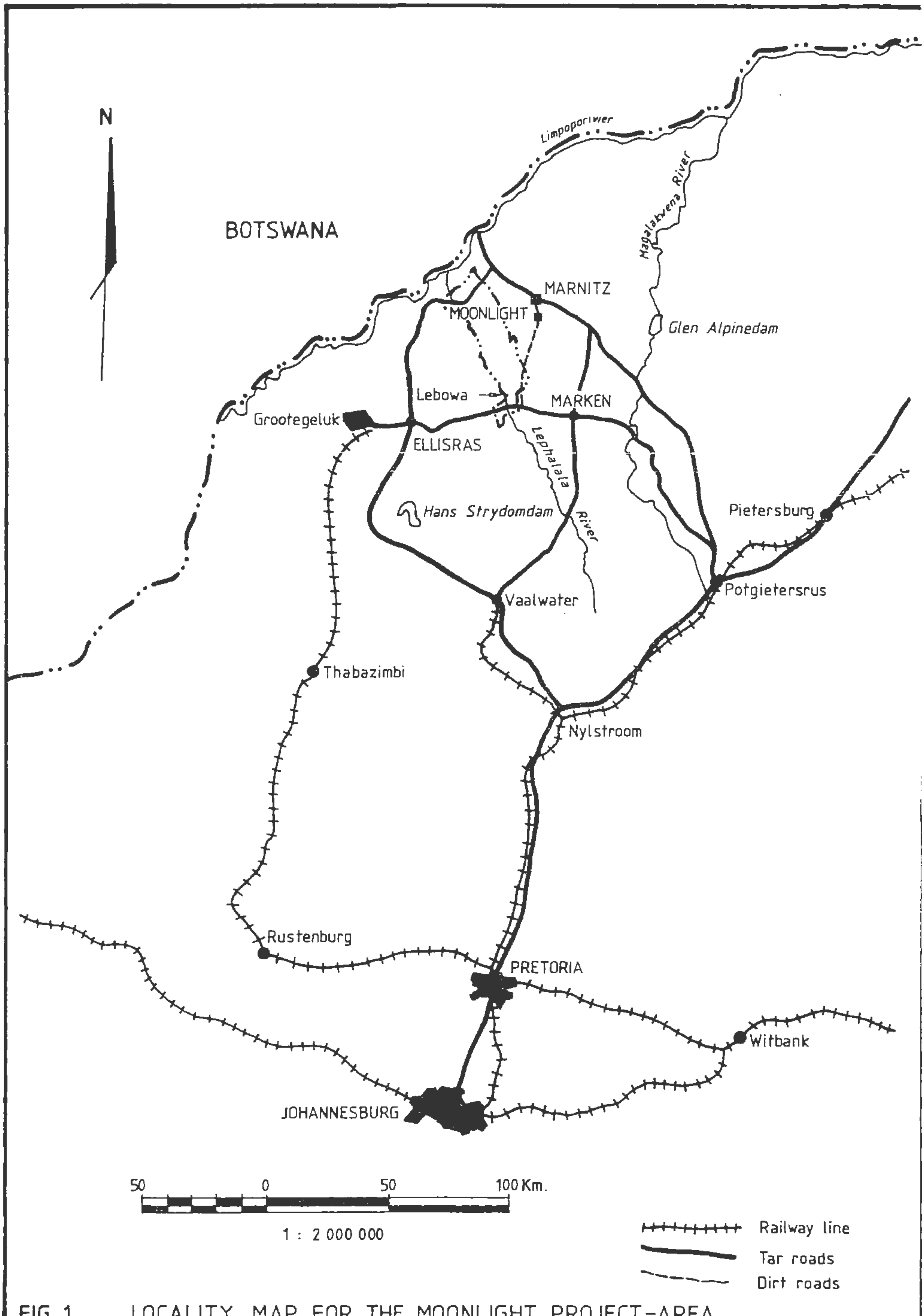

FIG. 1 LOCALITY MAP FOR THE MOONLIGHT PROJECT-AREA

Rivers:	Palala	23 km west
	Mogalakwena	46 km east
	Limpopo	35 km north-west
Dams:	Glen Alpine	50 km west in Mogalakwena river

Large areas of Lebowa are situated within 12 km of Moonlight, and labour is thus available (fig 1).

1.3 PHYSIOGRAPHY

The Moonlight project-area is generally flat-lying and sand covered, with the vegetation comprising grass, shrubs and big trees (mainly Maroela and knobby thorn - plate 1). Certain plant species or combinations thereof are an indication of the underlying lithologies or depth of overburden, eg Acacia Senegal which are found on the magnetite-quartzite outcrops and suboutcrops. Areas where calc-silicates of the Gumbu Group suboutcrop, are covered by calcrete and are thus sparsely vegetated. Acacia Senegal, Acacia Tortilis, Boscia Foetida and thorny shrubs are typical plants found in the calcrete-covered areas.

Plate 1 A tree-top view over the Moonlight project-area with the Koedoesrand in the background

1.4 EXPLORATION METHODOLOGY

The exploration programme was initiated by a management request to identify, procure and evaluate long-term iron ore reserves. The initial exploration programme planning included detailed literature surveys, the compilation of all existing data on iron ore deposits, and the selection of target areas from regional geological and aeromagnetic maps.

Target areas (eg Moonlight) were defined and more detailed geological surveys conducted. These included air photo interpretation and detailed geological mapping, ground-magnetic surveys (Plate 2) and trenching.

Plate 2 Part of the ground magnetic survey team

Percussion and diamond-drilling (Plate 3) followed in selected areas on Moonlight, with drill positions chosen from results obtained from the ground magnetic survey. It can be seen from map 2 (in back pocket) that valuable information regarding the structure and depth extension of the orebodies could be obtained from the geomagnetic survey.

Plate 3   Diamond drilling on grid positions

The success of aerial and detailed geological mapping were limited due to the scarcity of outcrop and the thick sand cover over most of the area. Interpretation of the geology in trenches was problematic due to big boulders and magnetite quartzite scree around outcrops and suboutcrops.

A small percussion drill was used to determine the continuity of suboutcrops and in delineating the shallow ore up to 50 m depth. It was also found that weathering extended down to 50 m below surface and that practically no core was recovered within this interval. In many cases, percussion holes had thus to be drilled in the same position as diamond boreholes, in order to obtain meaningful results.

Water levels in percussion boreholes were monitored on a regular basis as part of a geohydrological study conducted to evaluate the groundwater in the area as a source for supply to a possible mine. A grid of 200 m x 300 m was drilled with diamond drillholes, as well as one north-south and one east-west detailed-line on a 100 m borehole spacing

(Map 1 in back pocket). This was drilled in order to obtain a better control on the complex structure of the orebodies and to determine the quality and continuity of the orebodies.

Detailed sampling together with chemical and mineralogical investigations were conducted on drill-core from the ore-zones and associated lithologies, and beneficiation tests were carried out on composite samples from the ore-zones.

An evaluation of all the results obtained from the abovementioned exploration activities enabled the company to make a sensible decision on whether or not to exercise the mineral rights options.

2. REGIONAL GEOLOGY

The Moonlight magnetite-quartzite and associated lithologies represent Archaean metasediments, gneisses and intrusive rocks of the Limpopo Belt which have been complexely folded and refolded and which have at the same time been transformed and recrystallized under conditions of extreme metamorphism.

The igneous and high-grade metamorphic rocks of the Limpopo Belt are situated between low grade granite-greenstone terranes of the Kaapvaal and Zimbabwe cratons. The Limpopo Belt extends for over 700km in length and up to 200km in width, and is covered by Kalahari sands in the west and Proterozoic and Phanerozoic cover in the east (figure 2). Tankard et al (1982) divide it into: a Central Zone with a well developed supracrustal sequence (Beitbridge Complex) that has been metamorphosed to granulite and amphibolite facies and deformed into large north-trending periclinal structures; two marginal granulite Zones (Southern and Northern Marginal Zones) containing large proportions of

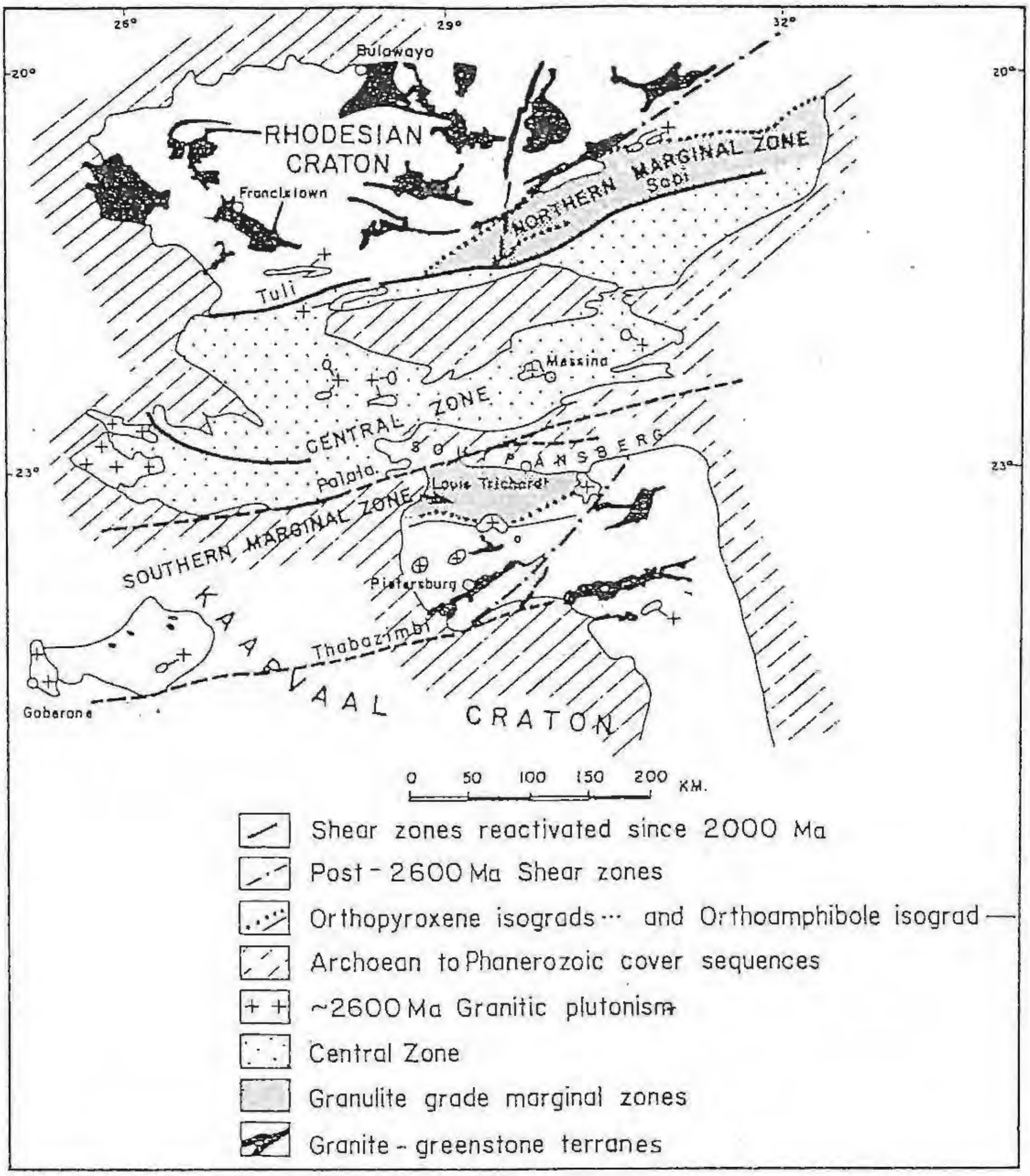

Fig 2 Tectonic zones within the Limpopo Belt and their relation to granite-greenstone terranes of the adjacent Zimbabwe and Kaapvaal Provinces (Du Toit et al, 1983)

deformed granitoids and subordinate precratonic cover sequences of greenstone affinity, that have been deformed into strongly linear or periclinal structures parallel to the margins of the zones. The Northern and Southern Marginal Zones appear to be reworked and metamorphosed granite-greenstone terranes which are separated from the Central Zone by ENE-trending late Archaean shear zones.

The Moonlight lithologies are correlated with the Central Zone of the Limpopo Belt on the basis of the following points:

1. The lithologic units present at Moonlight are identical to those in the Central Zone to the north and north-east, and differ markedly from those in the Southern Marginal Zone as described by Du Toit et al (1983).

2. The outcrop pattern of the Koedoesrand area indicates dome and basin structures similar to those in the Alldays-Messina area of the Central Zone (McCourt, 1983).

Due to complex deformation, the absence of marker horizons, the lack of outcrops with lithological relationships, and the highly metamorphosed character of the lithologies, no stratigraphic succession could be recognized at Moonlight. When compared to the lithostratigraphic units described by SACS (1980) and Brandl (1983), the magnetite quartzites at Moonlight have to be classified as part of the Mount Dowe Group, Beit Bridge Complex. Calc-silicate rocks of the Gumbu Group crop out to the north and south of the magnetite quartzites and join up in a large-scale fold-nose to the west (figures 3 and 4).

The lithostratigraphy of the Sand River Gneiss and the Beit Bridge Complex of the Limpopo Belt, are summarized in table 1. The Sand River Gneiss is regarded as basement to the supracrustal and intrusive rocks of the Beit Bridge Complex, although this proposed basement-cover relationship cannot be corroborated by field evidence (Van Reenen and Roering, 1990). Of all the different lithological units, only rocks from the Mount Dowe, Malala Drift and Gumbu Groups and the Messina Suite were recognized in the project-area.

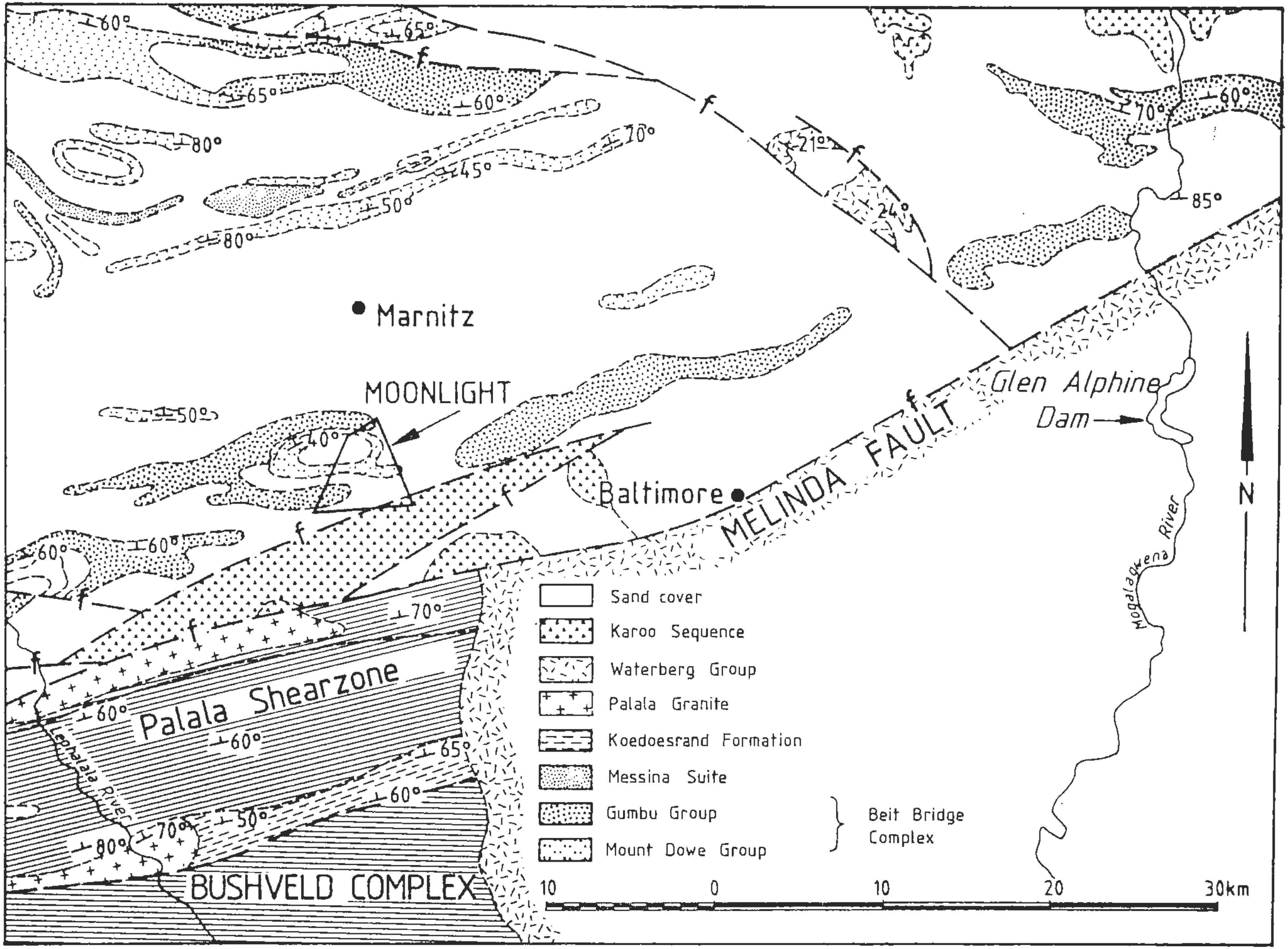

FIG. 3 GEOLOGY OF THE KOEDOESRAND AREA (Mc COURT 1983)

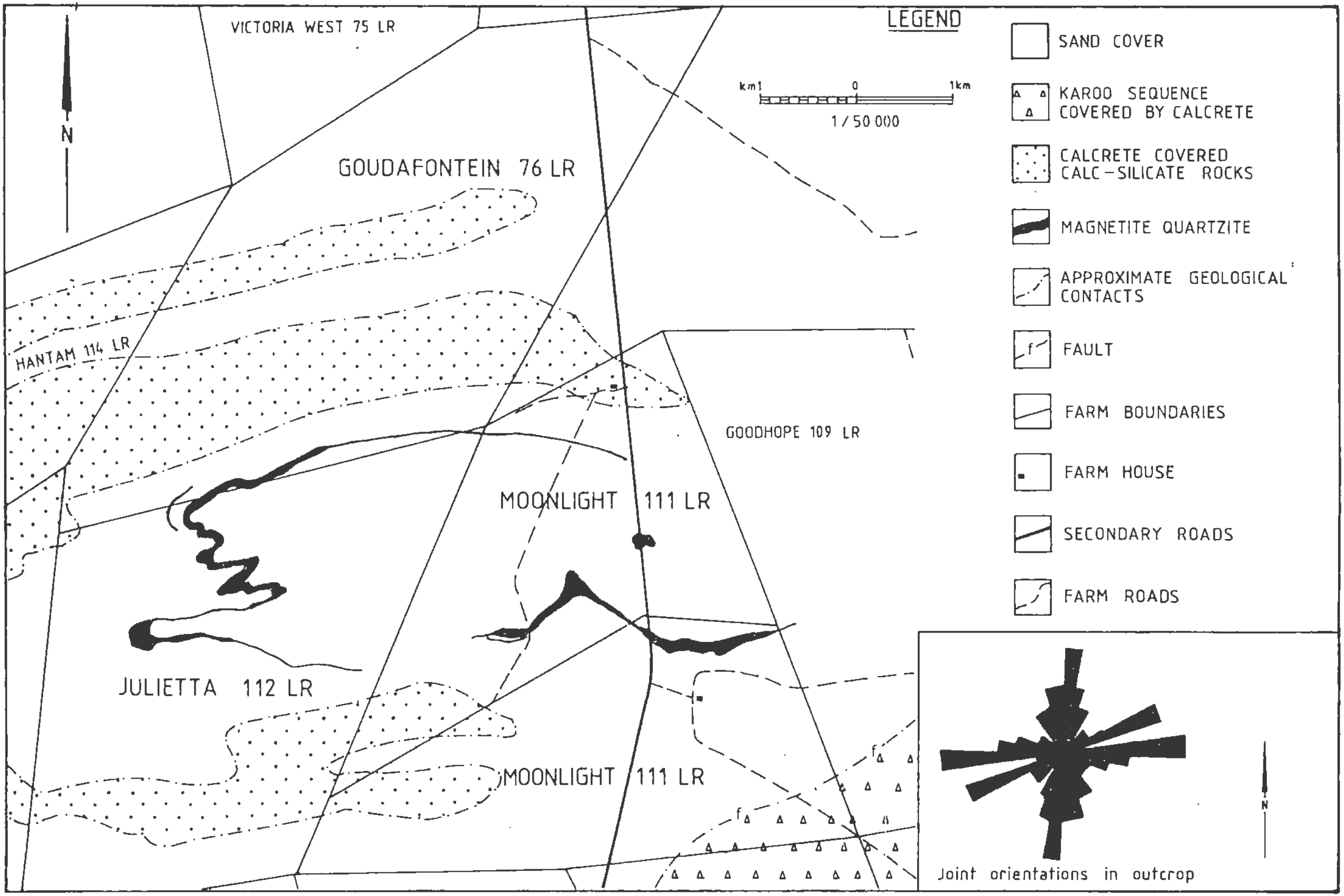

FIG. 4 SURFACE GEOLOGY OF THE MOONLIGHT PROJECT AREA AND SURROUNDING FARMS.

Table 1 Lithostratigraphy of the Sand River Gneiss and the Beit Bridge Complex (SACS, 1980)

		Lithology	Thickness (m)	Age (Ma)	Intrusives
Beit Bridge Complex	Bulai Gneiss	Grey porphyroblastic biotite gneiss of tonalitic composition			Bulai Gneiss 2 772±106 Ma[x]
	Messina Suite	Anorthosite and leuco-gabbro with gabbro, chromitite and titaniferous magnetite; sepentinite, metapyroxenite, hornblendite		3 153±47[xx]	
	Gumbu Group	Calc-silicate rocks and marble with leuco-gneisses, pink hornblende granitoid gneiss, metaquartzite, amphibolite - garnets common	~500		
	Malala Drift Group	Leuco-gneiss with metaquartzite, pink hornblende granitoid gneiss, amphibolite, metapelite, calc-silicate rocks	~1 000		
	Mount Dowe Group	Metaquartzite with leuco-gneiss, magnetite quartzite, pink biotite-hornblende granitoid gneiss (Singelele Gneiss), amphibolite, metapelite, calc-silicate rock-	> 1 000	Singelele Gneiss 2 509±260[x]	
Sand River Gneiss		Migmatitic grey and leucocratic gneisses - hypersthene-bearing, of granodiorite composition		3 858±116[x]	Tholeiitic dykes of 3 128±81[x] and 3 643±102 Ma[x]

For references to ages: [x]Barton and Ryan (1977)
[xx]Barton et al. (1978)

3. SURFACE GEOLOGY

The project-area is to a large extent sand-covered with few and widely spaced outcrops consisting mainly of magnetite quartzite (MEQ). Pink coloured dolomitic limestones of the Gumbu Group crop out in the south-western corner of Moonlight and calcrete covered calc-silicates are found along the northern border of the farm (fig 4). Calcrete in the south-eastern corner of the project-area overlies Karoo Sequence rocks, which are faulted down into lithologies of the Central Zone.

Plate 4 Magnetite quartzite outcrop on Moonlight IIILR

Magnetite quartzite scree and pebbles are widespread throughout the area especially around magnetite quartzite outcrops or suboutcrops. Due to the scarcity of mapable units the distribution of scree and pebbles were also mapped (Map 1, in back pocket), and proved valuable in determining the suboutcrop positions of the orebodies. The disadvantage of the scree cover was that it complicated the mapping of outcrop and that it produced magnetic anomalies whether or not it was associated with magnetite quartzite suboutcrop.

4. LITHOLOGIES

In this chapter the lithologies and their relationships to each other will be described briefly, with some mention of geochemistry and petrography.

Although no stratigraphic sequence could be established for the Moonlight lithologies, and because it is known that some or all of the MEQ-orebodies could be duplications of a single supracrustal iron-formation deposit, a generalized stratigraphic column was drawn up to illustrate the relationship between the different lithological units and to show the relative positions of the different MEQ-orebodies to each other (fig 5).

4.1 BASEMENT GNEISSES

These gneisses (Sand River Gneiss) as described by Horrocks (1981) and Watkeys et al (1983) were not recognized in the study-area. Two main varieties have been described. A migmatitic gneiss which consists of medium-grained, alternating layers of a mesocratic quartz-diorite and a leucocratic granodiorite. The second variety, a banded gneiss, has sharp contacts between the layers of medium-grained mica-quartzdiorite and slightly coarser, leucocratic granodiorite or adamellite. Most of these lithologies are hypersthene-bearing and of granodioritic composition. Barton et al (1985) obtained a Rb-Sr whole-rock isochron of 3 786 ±61 Ma for the Sand River Gneisses, although this dating is heavily disputed at present. Harris et al (1987), for example, give a maximum Nd-model age of 3200Ma to the Sand River Gneiss. 3200 Ma is regarded to be closer to a minimum age for the Sand River Gneiss, because the Messina Suite rocks (3150 Ma) were emplaced into the supracrustal lithologies which were deposited on the Sand River Gneiss basement.

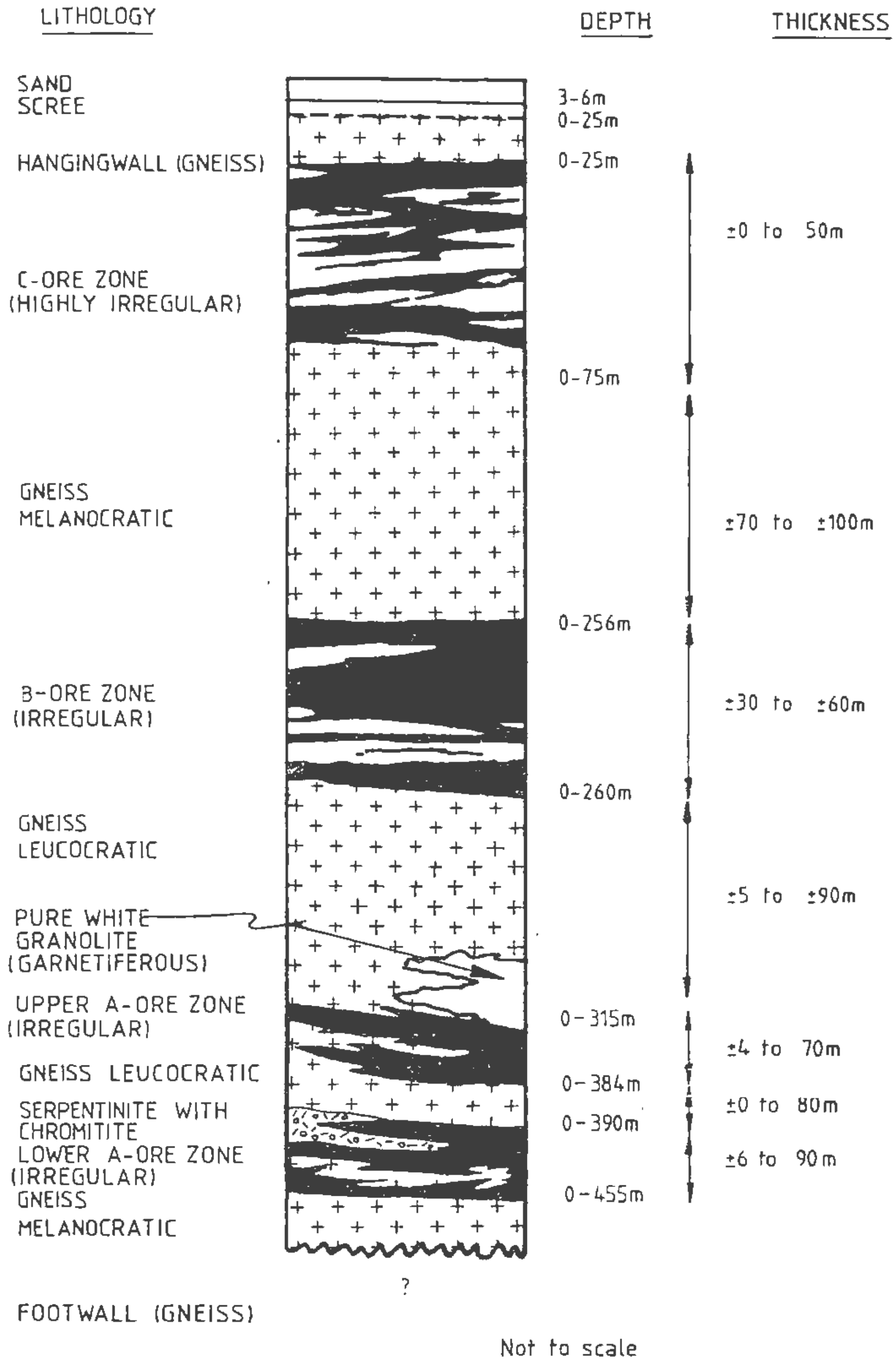

FIG.5 A GENERALIZED STRATIGRAPHICAL PROFILE OF THE MOONLIGHT MEQ-ORE BODIES.

4.2 SUPRACRUSTAL LITHOLOGIES

All rocks considered to have been deposited onto the basement gneisses are herein termed supracrustal lithologies (Beit Bridge Complex). The volumetrically dominant rock-types in the project-area are a variety of leucocratic quartzo-feldspatic gneisses which are typically strongly foliated and display well-developed metamorphic banding. The exceptions to the rule are the different granulites which possess granoblastic textures, and to a certain extent the magnetite quartzites (ferruginous granulite) which in some cases show remnant sedimentary layering.

4.2.1 Gneiss

Because no stratigraphic sequence could be recognized at Moonlight, the different gneissic lithologies are lumped together under the general term gneiss. Most of the gneisses can be described as quartzo-feldspatic gneiss although varying amounts of dark minerals are present, and may be the main constituent. The different lithologies are classified on the basis of the dominant mafic mineral present, and are described seperately, excluding the granulites which pertain to those lithologies with a characteristically granoblastic texture. The majority of the gneisses are strongly foliated and display prominent metamorphic banding. Many of the feldspars are intensely sericitized, whereas hornblende and biotite are often replaced by chlorite and to a lesser degree by epidote. It is difficult to determine whether most of the gneissic lithologies are para- or orthogneiss, but at Moonlight, abundant metapelites with almandite garnets are recognized, which probably points to a sequence consisting mainly of para-gneiss.

Hornblende gneiss

The hornblende gneiss is a grey to green-coloured rock and comprises hornblende, oligoclase/andesine, microcline and quartz (Plate 5). Subordinate amounts of biotite, chlorite and pyrite are present with the chlorite replacing biotite. Trace amounts of zircon and apatite are found, and cross-cutting quartz-feldspar veins may be present. A pronounced mineralogical banding is sometimes present, with layers consisting almost exclusively of hornblende, with subordinate amounts of biotite and plagioclase, alternating with coarse-grained biotite-hornblende-microcline plagioclase layers, containing subordinate amounts of quartz.

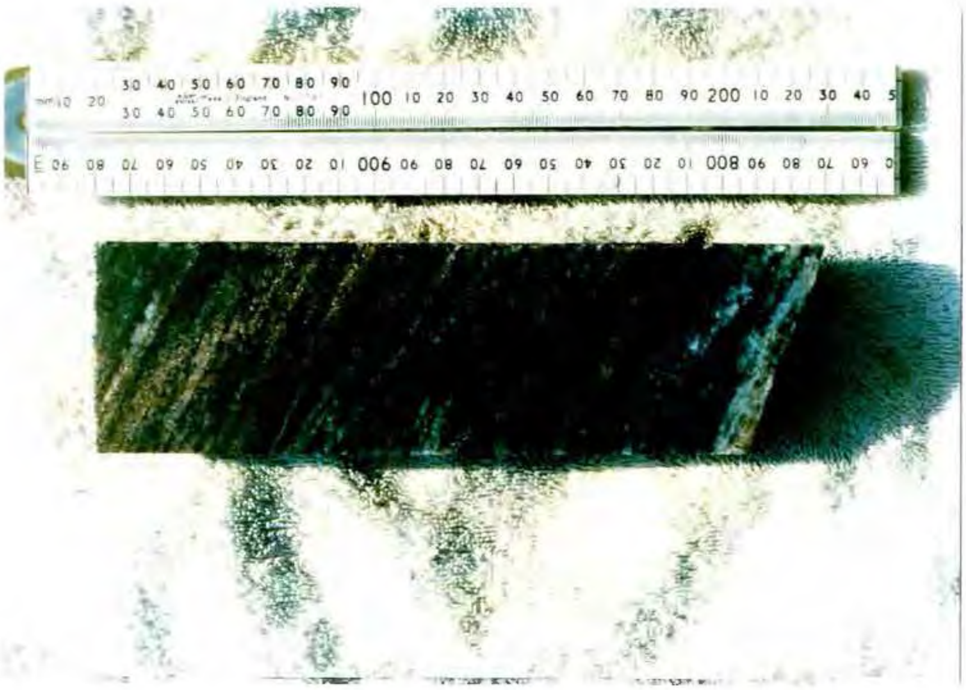

Plate 5 Hornblende gneiss in a drill-core sample

Biotite and garnet gneiss

Biotite gneiss is represented by a dark-grey, medium-grained rock which consists of quartz, albite/oligoclase, microcline, biotite and chlorite, whereas almandite and muscovite may be present in subordinate amounts. Coarser-grained more mafic varieties with pelitic compositions are also found with garnets up to 5 mm in diameter, which may constitute a major part of the gneiss (garnet gneiss). They are generally interlayered and infolded with the quartzo-feldspatic gneisses, and are regarded as the most important rock-type in the study of the metamorphic evolution of the Limpopo Belt. The use of almandite and cordierite as P-T indicators is well known (Winkler,1973).

Chlorite gneiss

Chlorite gneiss, a pink-coloured medium- to coarse-grained quartzo-feldspatic gneiss, is widespread throughout the project area, with chlorite present as a retrogressive metamorphic product of biotite and/or hornblende (Plates 6 and 9). It's main constituents are quartz, plagioclase (oligoclase, severely sericitised) and lesser amounts of chlorite. Apatite, hornblende, magnetite, allanite and zircon may be present in accessory amounts, whereas calcite is found mainly in cross-cutting veins. The gneissic character of the rock is prominent and formed by the planar orientation of chlorite, which macroscopically can be seen to cluster in irregular streaks, thereby inducing a mineralogical banding.

Augen-gneiss

This is also a leucocratic quartz-feldspar gneiss but with prominent "augen" of orthoclase (up to 3 cm) enfolded by chlorite, which might point to a pretectonic development of the feldspar. The augengneiss consists mainly of parallelly arranged, elongated grains of quartz, plagioclase, alkali feldspar, chlorite and/or hornblende. Biotite, zircon, apatite, allanite and magnetite may occur in subordinate to accessory amounts.

The quartzo-feldspatic gneisses are interpreted as representing original arkoses, although some of them might have been derived from felsic volcanics.

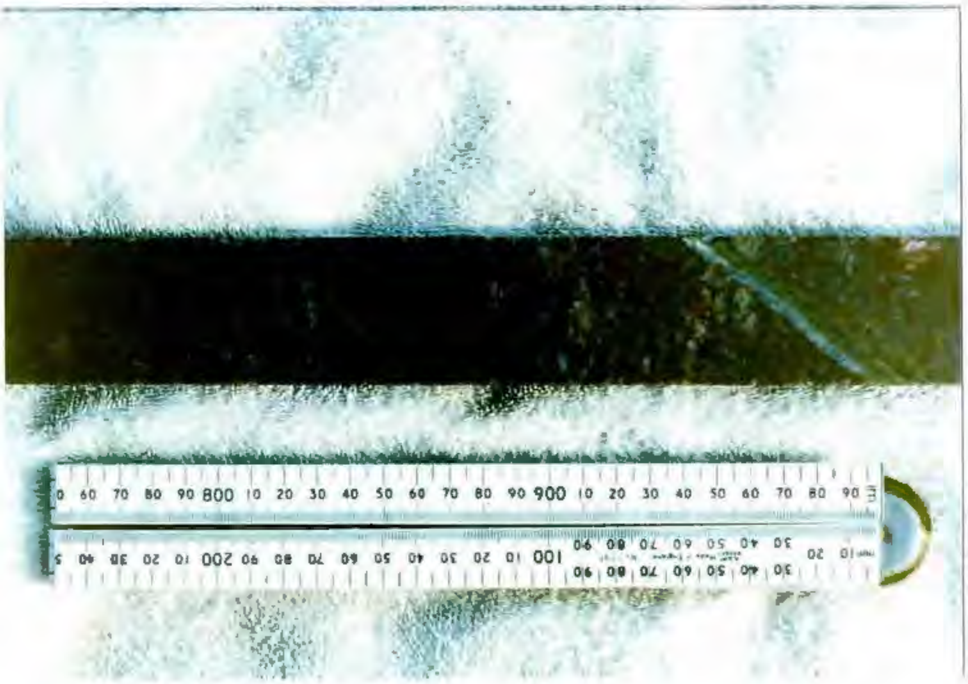

Plate 6 Chlorite-quartz-feldspar gneiss. Note the calcite vein along a fracture plane and epidote replacement on one side of the calcite vein

4.2.2 Felsic granulite

Under felsic granulite are included all the leucocratic lithologies which consist mainly of feldspar and quartz and which usually possess a xenomorphic-granoblastic texture. Perthitic microcline, sericitized plagioclase, and graphic intergrowths between quartz and feldspar are common.

Three main granulite varieties were identified in the Moonlight project-area viz:

(1) A pure white-coloured granulite consisting of quartz and feldspar only. It is medium- to coarse-grained, closely associated with the A-ore-zone in one area, and appears to be the metamorphic product of a psammitic rock (coarse-grained sandstone?). Fuchsite is commonly associated with the white granulite.

<u>Plate 7</u> Garnet-quartz-feldspar granulite.
The orientation of garnets in planes, may reflect remnant sedimentary layering or metamorphic banding

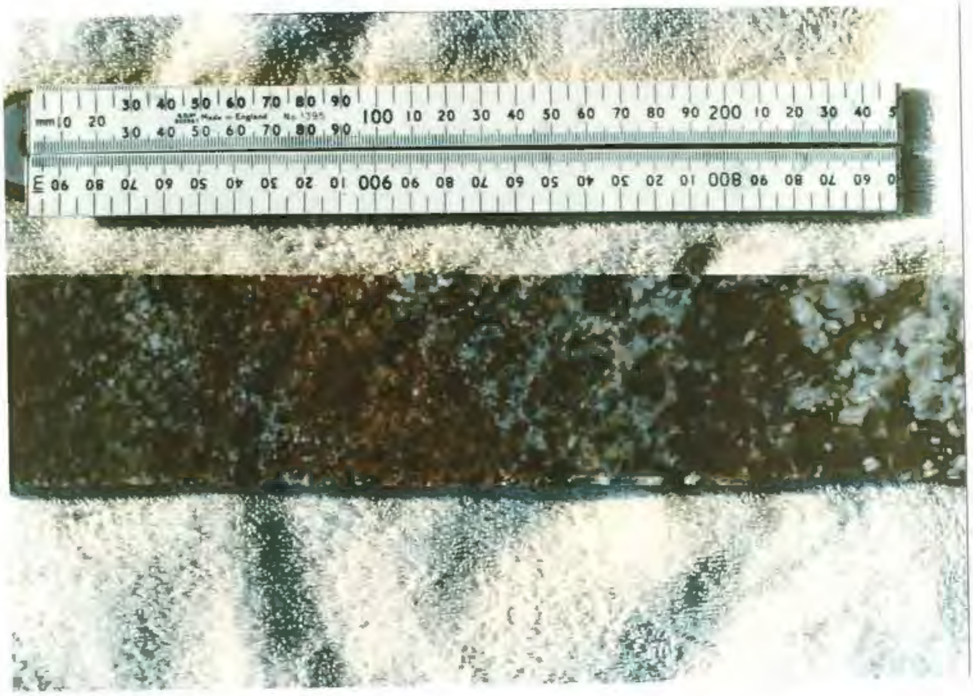

<u>Plate 8</u> Quartz-feldspar granulite with varying amounts of mafic minerals

(2) A medium- to coarse-grained quartzo-feldspatic granulite/gneiss with variable amounts of brown-red garnets (almandite) found along planes parallel to the regional foliation, or disseminated throughout the rock (Plate 7).

(3) Leucocratic, mostly pink-coloured granulites comprising of mainly quartz, and feldspar, but with varying amounts of mafic minerals which give the rocks a mottled appearance (Plate 8). Subordinate amounts of phlogopite, biotite, almandite, hypersthene, sillimanite, magnetite, Cr-spinel and retrogressive chlorite may be present. Composite-layering is developed in some instances, parallel to the metamorphic foliation and due to the segregation of felsic and mafic minerals.

The granulites may represent recrystallized partial melts of paragneiss, metapelites or felsic intrusives.

4.2.3 Magnetite quartzite

A variety of ferruginous granulites, notably magnetite quartzite (plate 9) are intercalated with the paragneisses. They vary in thickness from less than a metre to over 60 m, although it is difficult to determine whether or not the thicker horizons are duplicated by folding and/or thrusting. The magnetite quartzites may either terminate sharply along strike or down dip (due to boudinaging, isoclinal folding or original facies change), or pass laterally into increasingly iron-poor quartzite or even rare calcareous lithologies (dolomite) as seen on the farm Magdala, east of Messina. Magnesite is also found at Magdala as earthy masses and irregular veins in close association with the magnetite quartzite.

Plate 9 Magnetite quartzite and associated lithologies as seen in drill-core

Throughout the Limpopo Belt, internal banding is depicted by alternating layers, 1-20 mm thick, of medium- to coarse-grained magnetite and quartz. At Moonlight this banding is poorly preserved due to metamorphism which resulted in the magnetite quartzites being recrystallized, and mostly displaying a granoblastic texture. A weakly developed fabric defined by lengthened and flattened magnetite and quartz grains (L1-lineation) as well as thin zones of recrystallization/remobilization were noticed, which is tentatively correlated with later structures along which small-scale displacement took place (plate 10). It is suggested that the lithologies were close to anatectic P-T conditions and that melting occured only in local areas which experienced pressure release (dislocation planes). Recrystallization followed after deformation and destroyed all signs of the dislocation planes.

Small-scale graded bedding has been identified by Watkeys et al (1983), who also state that complicated internal deformation, mainly as a result of boudinage or disharmonic folding, has disrupted the fine alternating layers of quartz and magnetite. At Moonlight graded bedding is not recognized, but it may be due to the limited exposure of the magnetite quartzites. En echelon tension gashes along the limbs of folds have been infilled by white vein quartz and by remobilized magnetite. In fold noses one can also see concentrations of mobilized quartz and magnetite (plate 11), indicating again that local remobilization took place during deformation subsequent to the main deformational event (D1).

In addition to magnetite and quartz which comprise the oldest minerals within the magnetite quartzites, other minerals present include:

actinolite, hornblende and hastingsite:	<5%
plagioclase, K-feldspar, chlorite and calcite:	0-5%
talc, garnet, epidote, apatite, grunerite, sulphides, titanite and smectite:	<1%

Amphibole and chlorite are usually found concentrated on the contacts with adjacent lithologies, and pegmatite and dolerite are found as late intrusives (plate 12).

Hematite, martite, goethite and limonite are found mainly as oxidation products of magnetite in the weathered zone (up to 50 m depth).

On average, the magnetite quartzite at Moonlight contains 35% Fe (total), with a spread of 15% - 52%, and with a marked increase towards fold closures. Secondary iron-ore bodies containing more than 60% Fe are present in other parts of the Limpopo Belt, suggesting that local higher grade ores may also be associated with the Moonlight magnetite quartzites.

There is little doubt that the magnetite quartzite represents high-grade metamorphic equivalents of banded iron-formations similar to those of the flanking greenstone terranes. The very low TiO_2-content of the MEQ also confirms its sedimentary origin. The most noticeable difference is the volumetrically smaller amounts of associated metalavas (ultramafics) in the Central Zone. In the Rhenosterkoppies belt, approximately 30 km north of Pietersburg, the iron-formations on the northern edge of the Kaapvaal Craton are associated with an extensive succession of metalavas.

Plate 10 Coarse-grained recrystallization zone in magnetite quartzite (medium-grained)

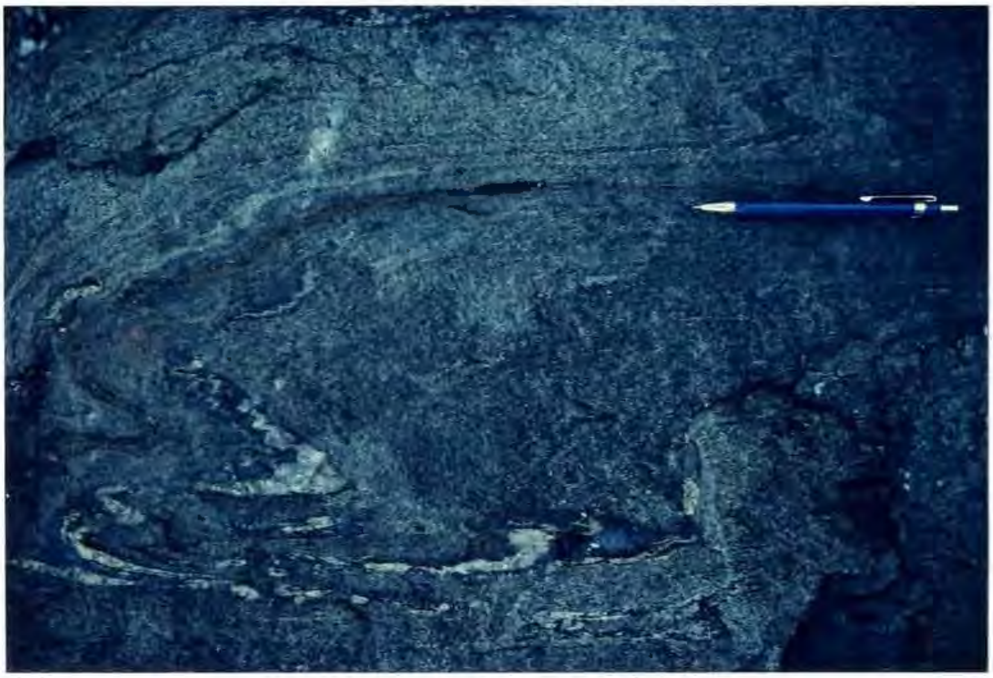

Plate 11 Fold structures in magnetite quartzite from the farm Randjesfontein, west of Messina. Note the concentrations of mobilized and recrystallized quartz and magnetite

PLATE 12 An intrusive pegmatite vein in magnetite quartzite

4.2.4 <u>Amphibolite</u>

Two main varieties of amphibolite were identified in the Moonlight-area, viz a banded, black, grey, or green coloured, medium-grained variety and a more massive, green coloured variety which is usually closely related to the magnetite quartzite ore, or the ultramafic lithologies.

The banded and foliated amphibolite occurs as concordant lenticular layers in the quartzo-feldspatic gneiss, and is composed of idioblastic hornblende and biotite, xenoblastic plagioclase and minor amounts of quartz. This variety is thought to represent a metamorphic product of shale, although the small amounts of quartz present, may point to basaltic volcanics as the original rock-type.

The massive, green-coloured variety is usually found conformable with the surrounding lithologies, but it may also cross-cut the banding and fabrics of the adjacent rocks.

Actinolite and hastingsite are the dominant amphiboles of the amphibolite in the magnetite quartzite, whereas actinolite, talc and diopside are the main minerals of the amphibolite within the ultramafic complexes. The cleavage pattern and relict crystal form of the talc is diagnostic of original orthopyroxene crystals. Subordinate amounts of calcite, chlorite and magnetite are found.

The massive amphibolite is interpreted as representing deformed mafic intrusives, except for the thin bands (<10 cm) within or on the contacts of the magnetite quartzite, which represent remobilized and recrystallized mafic minerals derived from metamorphic differentiation.

4.2.5 <u>Mafic-ultramafic complexes</u>

Three types of mafic-ultramafic complexes as described by Horrocks (1981) occur in the Limpopo Belt:

Type I: bands of serpentinite and metapyroxenite intercalated with the supracrustal rocks, especially the magnetite quartzites

Type II: pods of lenticular bodies of serpentinite and metapyroxenite in the noses of folds

Type III: sheets of meta-anorthosite to metagabbro/norite interlayered with the supracrustal rocks.

The first two types are considered as the "metapyroxenite-serpentinite suite" whereas the last type represents the "meta-anorthosite-gabbro suite". No outcrop of lithologies from these suites are present at Moonlight, but lithologies of the metapyroxenite-serpentinite suite were intersected during the drilling phase.

The ultramafic bodies appear to be lens- or pod-like in shape, and are present above, below or interlayered with the magnetite quartzites, especially the lower A ore-zone. Thicknesses of the ultramafic rocks intersected varies from less than 1 metre to approximately 50 metres, and the units usually have conformable relationships with the supracrustal rocks, with some of the thinner layers showing intrusive cross-cutting relationships on rare occasions. Larger bodies have complex internal layering defined by differences in composition, grain size and texture.

The dominant lithologies in the ultramafic units comprise serpentinite or carbonate-serpentinite with irregular lenses of pyroxenite, amphibolite, chromitite and lesser dunite. In hand sample the <u>serpentinite</u> and carbonate serpentinite appear relatively structureless, are brown, black, or green in colour, and may contain a wide variety of minerals. Serpentine (chrysotile, lizardite and antigorite), calcite, magnetite, hematite, magnesiochromite, diopside, tremolite-actinolite, talc and chlorite are the main mineral phases with lesser amounts of relict pyroxene and quartz. Calcite is also found as cross-cutting veins in the serpentinite.

A variety of textures are present, but the dominant texture seen is granoblastic-polygonal, after the original rock. Relict cleavage-patterns and crystal forms of both olivine and pyroxene occur.

Layers of pyroxenite and amphibolite up to 2 m wide, have gradational contacts with the serpentinite. The pyroxenite consists mainly of diopside and hornblende, with lesser amounts of quartz and magnetite, and accessory calcite and chlorite. The amphibolite (massive variety described under 4.2.4), comprises actinolite, talc and diopside.

Rare intersections of dunite (olivine rock) were found which appear to have escaped serpentinization.

Chromite occur in bands, schlieren or pod-like bodies of chromitite or disseminated in serpentinite. The chromitite horizons vary in thickness from a few millimetres to one metre, it is of low grade, very irregular and discontinuous. The chromitite present is mainly without structure, typically with a sugary texture, with the main mineral phase, xenoblastic to idioblastic magnesiochromite. Polygonal crystals of diopside and poikiloblasts of tremolite-actinolite are abundant, and calcite are found associated with pyroxene or as cross-cutting veins.
The Cr/Fe-ratio of the chromite is low at 1,1, and a microprobe investigation of the chromite gave the following approximate composition:
$(Mg_{0,3}.Fe_{0,9})(Cr_{1,1}.Al_{0,67})_2\ O_4$

Figure 6 represents part of a borehole intersection (MT37) through chromite-bearing lithologies, and depicts the whole-rock chemistry of the different lithologies. Chemographic relationships are depicted in figure 7.

The metapyroxenite-serpentinite suite as seen at Moonlight, represents an original intrusive rock with a peridotitic or pyroxenitic composition. This suite of rocks was thus intrusive into the supracrustal lithologies, although it is accepted that some of the ultramafic bodies may be reminiscent of the ultramafic extrusives associated with banded iron-formation of the Archaean greenstone belts. After emplacement, the ultramafic rocks were deformed and metamorphosed with the supracrustal sequence and have been remobilized into the noses of folds during tectonism.

The ultramafic complexes at Moonlight are classified as being part of the Messina Suite (Table 1), in spite of the fact that Horrocks (1983) observed a lack of spatial relationship of the serpentinite-pyroxenite units with the gabbroic and anorthositic rocks (TypeIII-complexes) in the Messina-Tshipise area. The latter are widely accepted as being part of the Messina Suite. The Messina Suite has been dated at 3150 Ma (SACS, 1980), and it was emplaced into the supracrustal lithologies which thereby places a minimum age of 3150 Ma to the deposition of the supracrustal rocks.

According to Light (1982), the parental magma of the Messina Suite is similar in composition to modern oceanic island arc tholeiites and to basalt from Canadian greenstone belts, and the magma can thus be interpreted as being derived from oceanic crust.

MOONLIGHT

BOREHOLE NO: MT37

APPROXIMATE SCALE 1:60

DATE: 15/11/90

LITHOLOGY DEPTH GEOLOGICAL DESCRIPTION

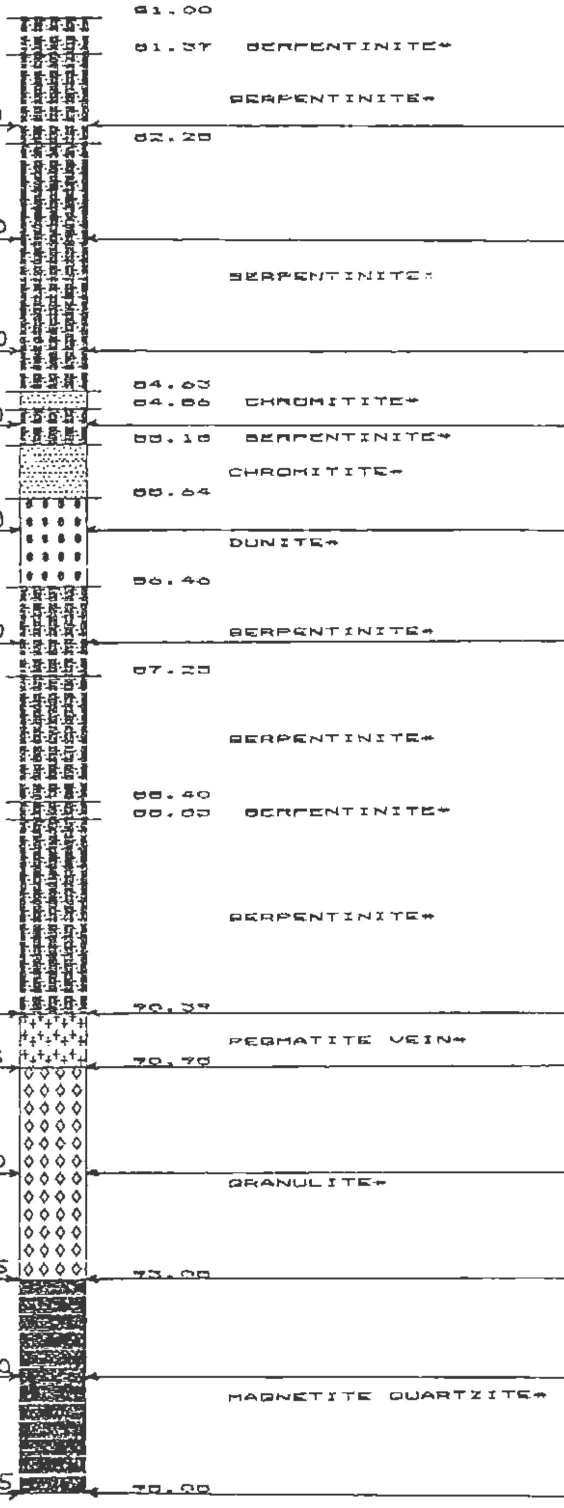

CHEMICAL ANALYSIS

Depth	SiO_2	TiO_2	Al_2O_3	Cr_2O_3	MnO	MgO	CaO	K_2O	P_2O_5	TOTAL Fe	TOTAL
82,10	28,56	0,06	3,32	7,63	0,45	27,64	10,32	0,02	0,14	7,5	80,7
83,00	36,02	0,05	2,72	4,76	0,41	26,78	11,22	0,01	0,11	6,6	86,3
84.00	27,00	0,14	5,92	17,14	0,65	14,66	10,98	0,01	,011	8,7	76,3
85,00	26,30	0,09	4,91	13,44	0,57	23,27	11,32	0,01	,011	8,0	77,6
86,00	25,94	0,14	7,65	22,26	0,65	16,06	12,09	0,03	,018	3,3	74,0
87,00	40,57	0,09	4,32	6,66	0,35	21,09	12,12	0,10	071	6,5	87,6
90,39	47,36	0,34	7,33	4,95	0,21	16,28	5,36	0,79	,149	8,4	88,7
90,96	85,03	0,10	4,46	0,30	0,01	2,78	0,62	1,16	,021	3,3	97,7
92,00	67,18	0,20	13,05	0,09	0,03	1,69	0,79	5,66	,234	4,7	89,6
93,05	64,09	0,28	13,43	0,03	0,01	0,64	0,60	5,47	,062	7,4	89,3
94,00	44,00	0,25	1,58	0,08	0,09	2,35	1,86	0,23	,117	33,8	97,1
95,05	44,74	0,17	1,80	0,10	0,06	2,17	1,42	0,40	,124	33,4	96,7

Fig 6 Geological column of part of a borehole intersection through an ultramafic complex. H_2O+ and CO_2 have not been reported, resulting in low totals for these samples

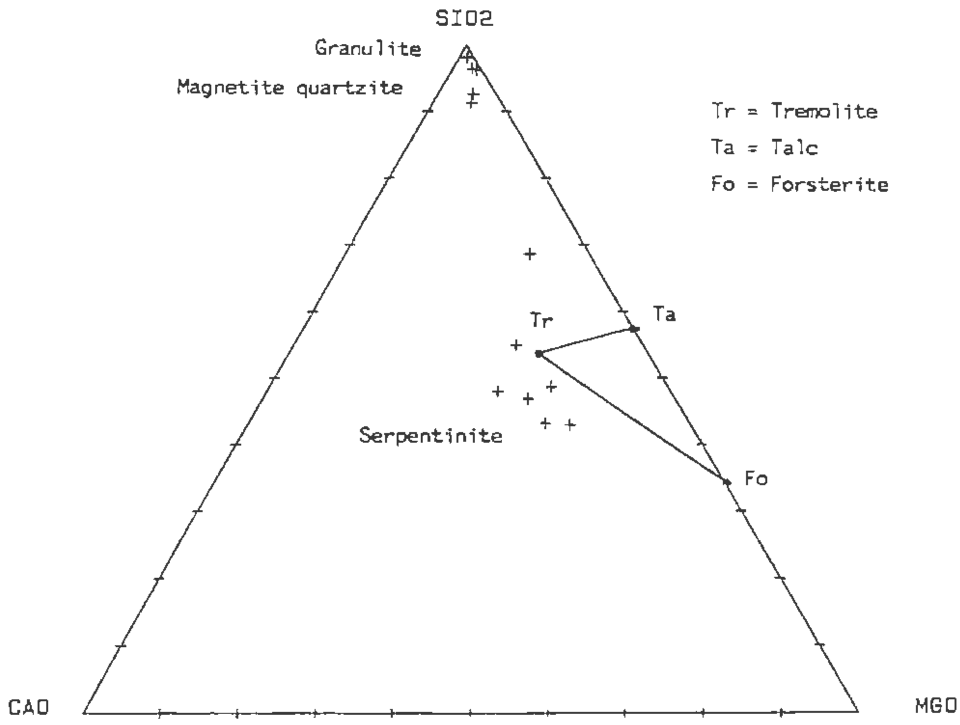

Fig 7 Chemographic relationships of the serpentinite and associated lithologies from borehole MT37

4.2.6 Mafic granulite

Mafic granulites are ubiquitous in most of the Moonlight drill-core, and display a wide variety of minerals, making it difficult to describe them as a single lithology. An example of one of the many mafic granulites present is described later in the text. These granulites may represent deformed and metamorphosed shale, mafic lava, dykes, plutonic rocks, or gneiss. The mineral assemblages consists mainly of plagioclase and pyroxene, with amphibole, quartz and mica present in varying amounts. Occasionally garnets have developed, sometimes displaying a corona of plagioclase and pyroxene or amphibole.

A drillcore sample from borehole MT47, at a depth of 184 m, illustrates one of these mafic granulites, and is a greenish grey, medium-grained metamorphic rock which consists mainly of diopside, hypersthene and plagioclase

(An40-50). Quartz, hornblende and magnetite occur in subordinate amounts, with accessory biotite, ilmenite, chlorite, hematite, pyrite, chalcopyrite, zircon, baddeleyite, scheelite and a Ni-telluride. The mineral assemblage and the granoblastic texture of the rock as well as the common but rarely twinned plagioclase are indicative of high-grade metamorphism of a probable mafic plutonic rock.

The granulite described, represents one of many which could not be classified as falling under a specific suite of rocks.

4.2.7 Metaquartzite

Only very thin and rare zones of metaquartzite are present in the Moonlight project-area, but they are found throughout the Limpopo Belt as prominent ridges with extensive talus-slopes. The metaquartzite is a massive, coarse grained white rock that often resembles vein quartz where recrystallized. Metamorphosed graded bedding has however been identified, arguing in favour of a sedimentary origin. Occasionally the metaquartzites are tinted green or reddish-brown by the presence of fuchsite or iron-oxides respectively.

Watkeys et al (1983) subdivided the quartzites into massive, fuchsitic, sillimanite-bearing and granular varieties. Sillimanite may develop along major partings representing bedding planes, along which quartz rods are often developed.

4.2.8 Calc-silicate rocks

Outcrops and suboutcrops of pink to grey-coloured calc-silicates and marble of the Gumbu Group are present in the Moonlight project-area and surrounding farms. The dominant lithology is calc-silicate with the composition of dolomitic limestone, which is white to grey in colour and medium- to coarse-grained. It is composed of calcite/dolomite with minor olivine, phlogopite, serpentine, amphibole, clinopyroxene, microcline, quartz and graphite. Locally more pure marble may be found, (Table 2) the extent of which is difficult to determine due to obscured lithological contacts. A pink-coloured, very fine-grained marble with up to 95,5% $CaCO_3$ was exploited as ornamental stone on the farm Holdrift, north of Moonlight.

The texture of the calc-silicates and marble vary between granoblastic equigranular polygonal and inequigranular interlobate. Original compositional layering is accentuated by strongly variable amounts of the minor constituents or by grain size differences.

The calc-silicates are closely associated with amphibolite and metaquartzite, and are intruded by pegmatite and dolerite.

Chemical analyses listed in table 2 show that the calc-silicates were originally dolomitic limestones and calcitic dolomites with only isolated occurrences of pure limestone. Dolomitization probably occurred after deposition.

4.2.9 <u>Late-intrusives</u>

<u>Diabase</u>

One thick diabase dyke (10 m - 50 m) and a few thinner ones were intersected at Moonlight (Map 3, in back pocket). In hand sample the rock is green coloured and fine grained with reddish K-feldspar <u>phenocrysts</u>. The reddish colour of the K-feldspar is caused by submicroscopic hematite. Albite represents the main mineral phase with augite, clinopyroxene, K-feldspar, and chlorite in subordinate amounts, with traces of magnetite, quartz and amphibole.

Table 2. **Chemical analyses of calc-silicate rocks and marble of the Limpopo Belt. The calc-silicates were only analyzed for elements which is of importance in limestone or dolomite when used as a flux in the steelmaking process**

Sample No	CaO	MgO	SiO_2	Fe_2O_3	MnO	Al_2O_3	TiO_2	K_2O
DT2	28,8	18,3	4,3	1,6	0,37	0,1	0,03	0,3
DT3	30,8	19,1	1,8	1,8	0,36	0,1	0,03	0,3
ZI2	41,6	7,8	2,5	0,9	0,33	0,3	0,02	0,30
AE2	45,8	6,5	5,1	0,8	0,15	0,2	0,03	0,50
AE9	40,9	10,9	10,2	0,6	0,06	0,1	0,03	0,4
CN1	40,7	1,9	20,2	2,8	0,06	5,2	0,19	1,8
IN1	50,0	1,9	3,8	0,8	0,32	0,4	0,04	1,4
RN1	50,9	2,9	1,9	0,64	0,10	0,1	0,04	0,1
DH1	27,8	16,8	5,75	2,2	0,88	1,20	0,08	0,54
DH4	44,5	2,4	7,39	0,8	0,17	1,8	0,09	0,66
DH6	46,1	2,3	5,42	0,8	0,18	1,5	0,07	0,56
DH11	47,5	3,3	4,58	0,6	0,07	0,1	0,01	0,01
DL5	47,9	1,4	5,83	0,6	0,09	0,8	0,07	0,40
DL17	29,6	17,8	4,66	1,33	0,39	1,2	0,06	0,11
HT18	30,8	21,2	1,11	0,42	0,08	0,22	0,01	0,13
ON1	30,2	21,1	0,72	0,93	0,40	0,22	0,01	0,04
ZN1	51,9	9,94	2,27	0,68	0,34	0,51	0,04	0,28
ZN3	52,9	1,43	2,04	0,64	0,39	0,52	0,04	0,06

Epidote and quartz veins are found within the diabase, with epidote also replacing the diabase in localized zones, especially along joint-planes.

The sack-name diabase is used for this rock-type although chemical analyses points more towards a dioritic composition (fig 8).

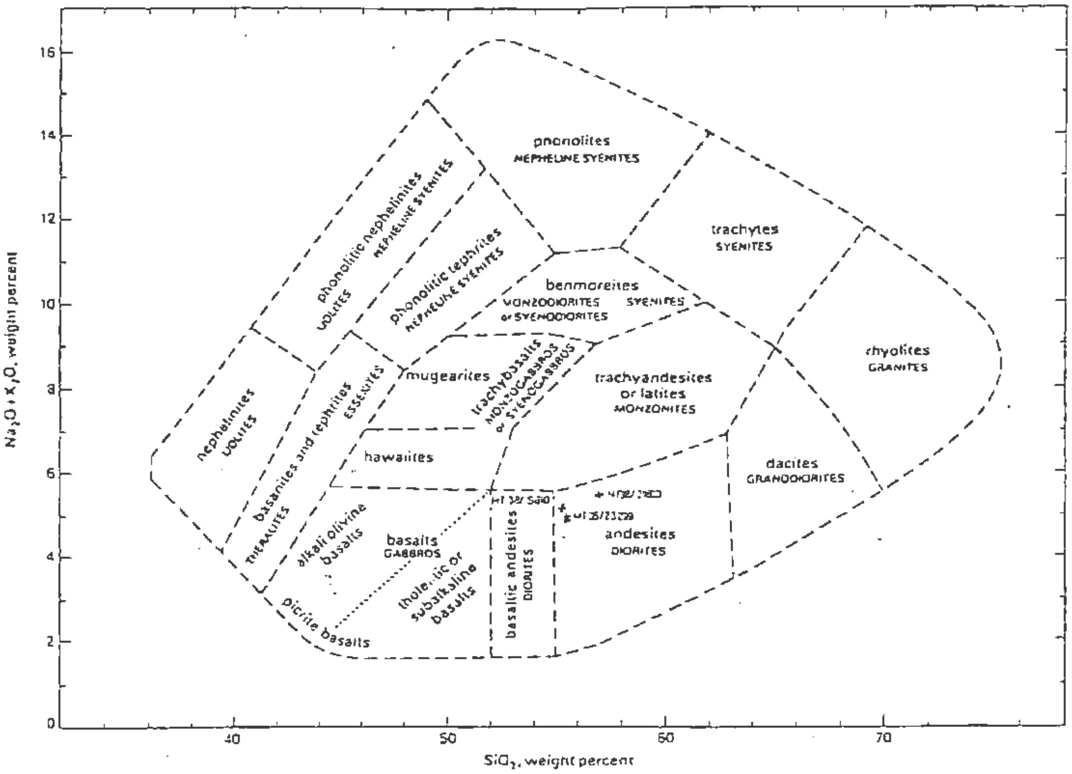

Fig 8 Diagrammatical illustration of the classification of igneous rocks (Mackenzie et al, 1982), with diabase-samples from Moonlight plotted in order to determine their chemical composition

Pegmatite

Pegmatite and aplite veins are ubiquitous in the drill-core from Moonlight, and vary from centimetre-scale to 15 m in thickness. They are usually found cross-cutting the foliation of the other lithologies, with dips of 10°-70° from horizontal.

The pegmatite is very coarse-grained, pink in colour, and consists of mainly subhedral alkali-feldspar, plagioclase and quartz. Graphic intergrowths between quartz and feldspar is common, and subhedral hornblende, biotite and magnetite are found.

4.3 GEOCHEMISTRY OF THE MOONLIGHT LITHOLOGIES

Whole-rock analyses were carried out on some of the lithologies in the project-area and are summarized in table 3. Due to the diversity of the different lithologies in this complex metamorphic terrain, the chemical analyses can never be fully representative of an average for the different rock-units. Stratigraphical units are also not accounted for.

Due to the economic importance of the magnetite quartzites, the population distributions of total Fe and the deleterious elements P, S and K_2O were plotted for the different ore-zones (Lower A, Upper A, B and C). The distributions for total Fe are illustrated in figure 9 and those for the deleterious elements in appendix 1. Two distictive Fe-populations exist for all the ore-zones, which represent the magnetite quartzite (ore) and the interbedded waste respectively. Most of the waste can still be mined on a selective basis, and will not lower the Fe grade significantly. Concentrations of the deleterious elements are very low and will pose no problem when these ores are used in the steelmaking process. See section 6.3 for a discussion on P, S and K_2O specifications for iron ore, and the effects of the deleterious elements on steel.

Like most other iron formations, the Moonlight magnetite quartzites have very low Al_2O_3, P_2O_5, Na_2O and K_2O values with MgO/CaO generally greater than 1. Their chemistry are very constant laterally and vertically except for the variation in iron- and silica-content. The B ore-zone eg in general has a higher Fe-content and a smaller spread of Fe-values than any of the other ore-zones, which can probably be explained by the migration of iron into the B-zone fold-closure during deformation (fig 19).

Polyphase metamorphism changed the mineralogy and thus the geochemistry of the different lithologies to such an extent that it is virtually impossible to determine the origin of the majority of the lithologies by means of geochemistry.

Host rock geochemistry will only became valuable in fingerprinting lithologies as soon as a stratigraphical sequence and/or units can be identified.

5. STRUCTURE AND METAMORPHISM

5.1 STRUCTURE

The rock units in the project-area are complexly folded and refolded on all scales. Aerial photos of the area show a general strike of 070°, which defines the mineral banding and regional foliation, that dips at 10° - 20° north at Moonlight. The dip of the foliation may change around fold-closures which is often the case on a regional scale, because of the presence of dome and basin type interference structures. The strike of the regional foliation (070°) is parallel to the Palala shearzone, a 10-12 km wide mylonite zone, 8 km to the south, which defines the southern boundary of the Limpopo Belt in this area.

Only isolated magnetite quartzite outcrops could be used for structural mapping at Moonlight, which made it extremely difficult to make any conclusive interpretations on the structure. Furthermore, no orientated drill-core was retrieved. This means that depth to intersection was used to establish the geometry of the magnetite quartzite orebodies and to interpret the local structure. From small-scale structures observed in outcrop and drill-core (fig 10), as well as regional observations, it is clear that the lithologies underwent a long and complex history of deformation and metamorphism. Watkeys et al (1983) described six deformational and metamorphic events, which was used as a guideline, although only some of these were recognized at Moonlight.

Table 3 : Chemical analyses of lithologies from the Moonlight project-area.

Weight %	1	2	3	4	5	6	7	8	9	10	11	12
SiO_2	55,85	58,34	58,89	67,03	73,77	30,17	58,27	44,38	49,26	51,80	67,67	37,22
TiO_2	0,90	1,06	0,30	0,46	0,36	0,08	0,34	0,87	1,21	0,68	0,51	0,04
Al_2O_3	13,89	10,78	7,51	14,37	10,52	4,56	21,64	15,23	13,00	18,22	14,37	0,34
Fe_2O_3	9,25	-	-	-	-	-	2,64	10,48	11,49	7,56	1,58	40,51
FeO	-	-	-	-	-	-	2,47	5,97	3.30	2,25	3,53	18,50
MnO	0,19	0.03	0,10	0,05	0,03	0,50	0,03	0,18	0,21	0,13	0,04	0,06
MgO	5,90	1,21	5,52	3,24	4,35	23,50	1,29	9,10	5,91	4,48	1,97	1,08
CaO	5,43	2,70	1,50	0,83	0,82	11,21	4,64	5,69	9,72	8,34	1,49	1,65
Na_2O	3,81	-	-	-	-	-	4,27	0,77	3,38	3,87	3,34	0,05
K_2O	1,59	0,71	1,97	3,32	1,38	0,02	1,95	2,84	1,49	1,64	3,48	0,05
P_2O_5	0,11	0.08	0,07	0,07	0,01	0,05	0,12	0,30	0,15	0,17	0,24	0,10
Cr_2O_3	-	-	0,07	0,07	0,53	11,55	0,03	0,04	0,03	0,02	0,03	0,05
Total Fe	-	14,50	13,93	4,43	4,20	7,47	3,70	11,90	10,70	7,10	3,70	42,70
Total	96,92	-	-	-	-	-	97,68	95,84	99,14	99,16	98,26	99,65

NOTES:

1. Diabase (Dioritic composition)
2. Pegmatite)
3. Biotite gneiss)
4. Chlorite gneiss) Average compositions of a
5. Hornblende gneiss) number of samples
6. Serpentinite)
7. Granulite)
8. Amphibolite)
9. Biotite gneiss) Analyses of single selected samples
10. Hornblende gneiss)
11. Chlorite gneiss)
12. Magnetite quartzite)

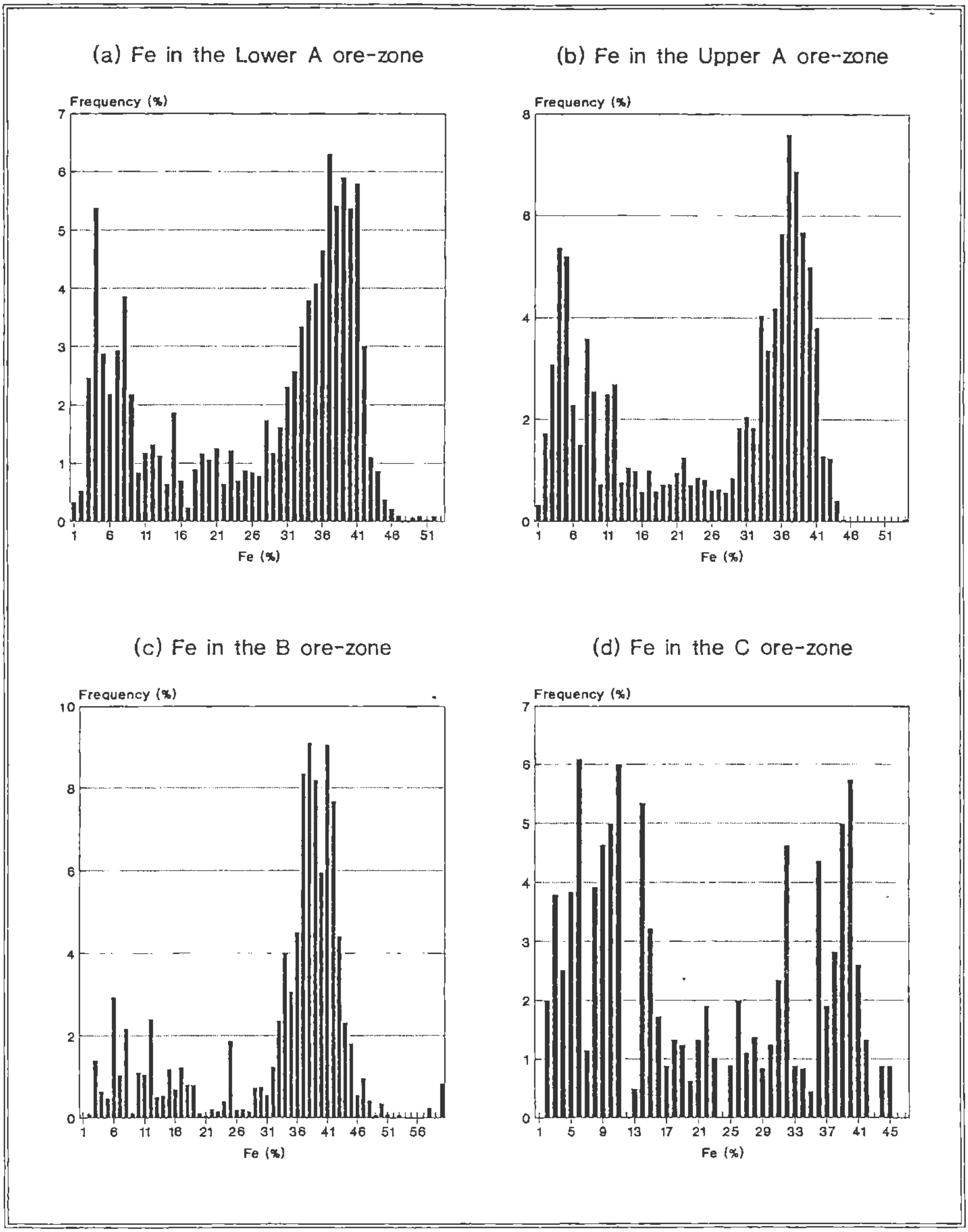

Fig 9 Frequency distributions of total Fe for the Lower A, Upper A, B and C ore-zones at Moonlight

In outcrop, the magnetite quartzites do show complex folding and a large scale synformal structure (sheath fold?) is present on the farms Moonlight, Julietta and Goudafontein (fig 4). More detailed studies in the Moonlight project-area however refute this observation because no lateral or in depth extension of the magnetite quartzite between the Moonlight and Julietta-Goudafontein areas was found. It is possible though that the two areas could have been linked by an eroded D2 antiformal structure.

Isoclinal folding is seen in drill-core and outcrop, and it is clear from the interpretation of the orebodies on the suboutcrop map and geological sections (Figures 11 and 12, and map 3, in back pocket) that isoclinal folding duplicated the magnetite quartzites. The isoclinal fold-axis plunges in a north-easterly direction at ± 20°, which corresponds to lineations measured on a regional scale (Van Reenen and Roering, 1990).

Small-scale structures observed at Moonlight (fig 10) are discussed below, in order to produce a better background to the final interpretation of the deformational history of the lithologies present.

In situ structures in <u>outcrop</u> are rare and widely spaced throughout the project-area, partly due to poor outcrop exposure. The vague banding in the magnetite quartzites, interpreted as original bedding (So), can be seen in outcrop together with a subparallel foliation (S1) defined by lengthened and flattened magnetite and quartz grains in magnetite quartzite and the orientation of dark minerals in the gneissic lithologies (regional foliation). Stretching lineations defined by the lengthened magnetite and quartz crystals, plunge at 20° in a direction 047° at Moonlight. On the farm Julietta mineral lineations were observed, which plunge at 36°-40° in a north-northwesterly direction.

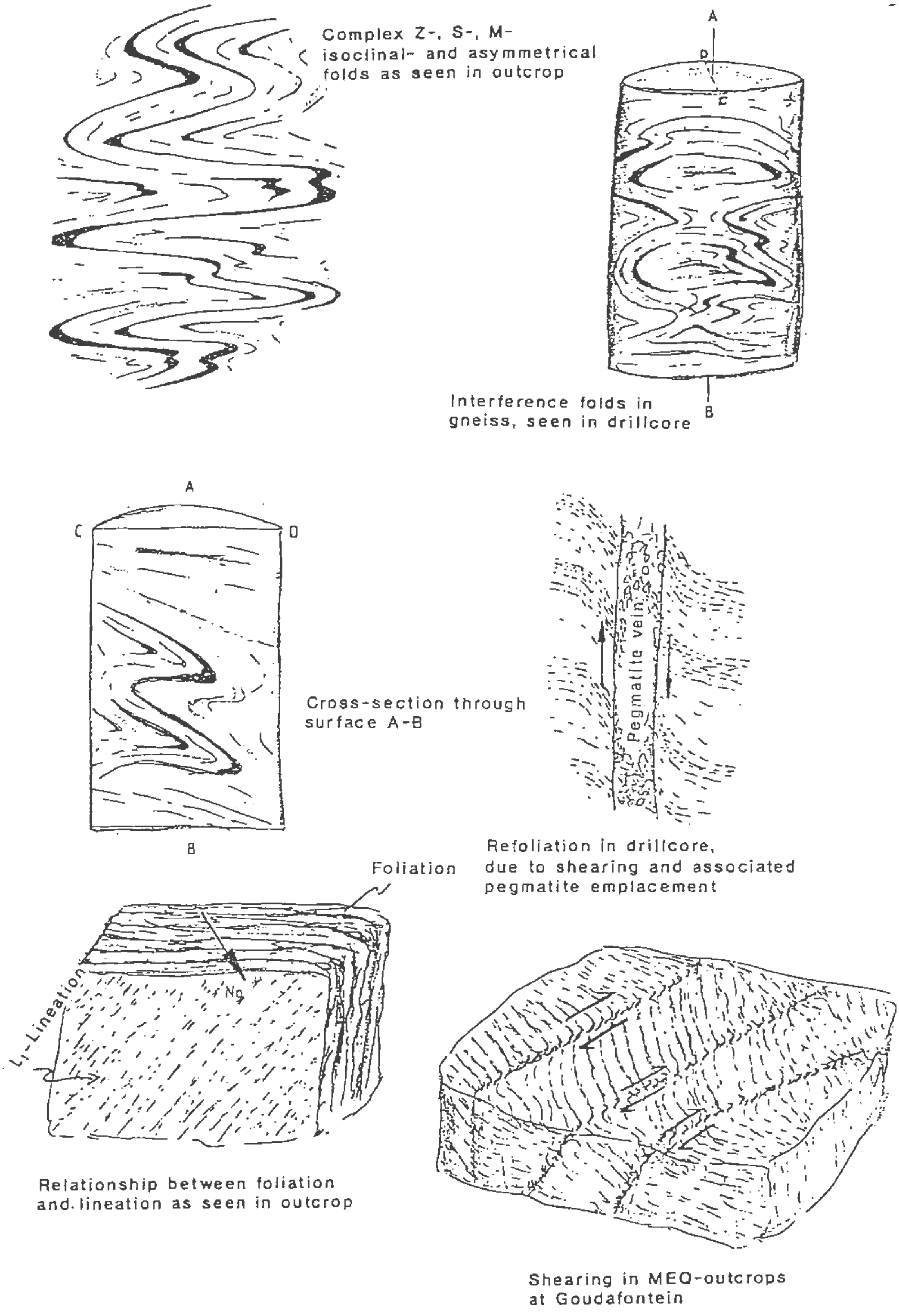

Fig 10 Small-scale structures as observed in outcrop and drillcore

This discrepancy in the same set of mineral lineations is difficult to explain because no detailed work was carried out in the Julietta area, and reliable lineations for the purpose of structural mapping are rare throughout the project-area. The most probable explanation would be that the D1-lineation was refolded during the subsequent D2-deformation.

Small-scale folding (S, Z, and M) is present in magnetite quartzite outcrops, especially in larger scale fold-closures. Recrystallized magnetite quartzite and associated higher grade ores are locally found in these thickened zones. Small-scale shear-planes with associated refoliation zones
were observed on Goudafontein. Displacement on a single shear-plane never seems to be more than 3 cm. Tension gashes with quartz growth parallel to the direction of maximum extension are also found in this area.

Slickensides are ubiquitous throughout the area, along joints filled with quartz or limonite. The most prominent joints in outcrop are related to post-Karoo deformation, because their orientations coincides with joints in Karoo lithologies in the area. See the Rose diagram in figure 3 for joint orientations measured in outcrop.

Small-scale folds as well as interference structures are abundant in drill-core, especially in the gneissic lithologies. Folds which have been completely disrupted as a result of very strong elongation after their formation are common and are defined by sickle-shaped leucocratic fold-closures.

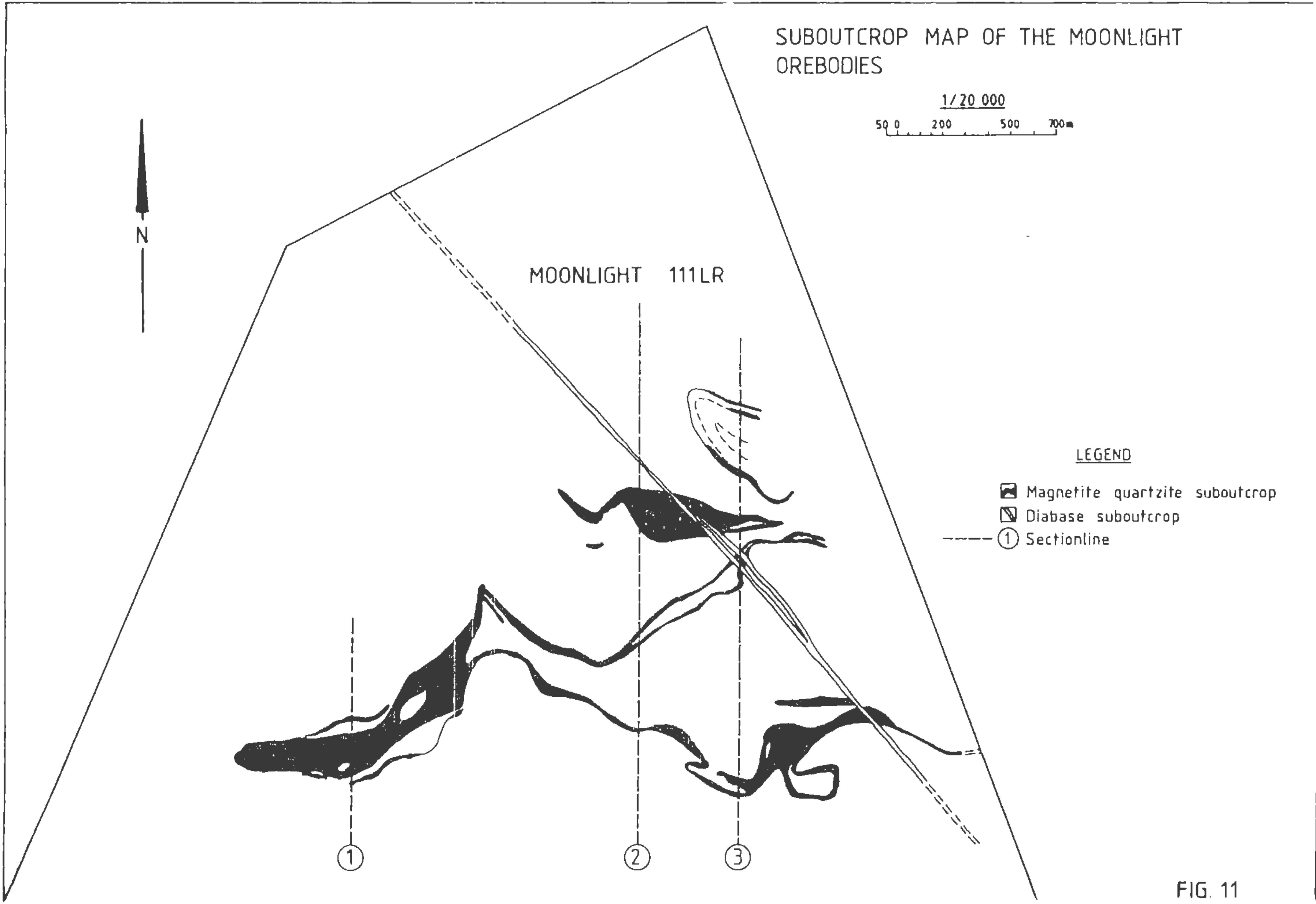
SUBOUTCROP MAP OF THE MOONLIGHT OREBODIES
1/20 000
50 0 200 500 700m
N
MOONLIGHT 111LR
LEGEND
Magnetite quartzite suboutcrop
Diabase suboutcrop
1 Sectionline
1
2
3

FIG. 11

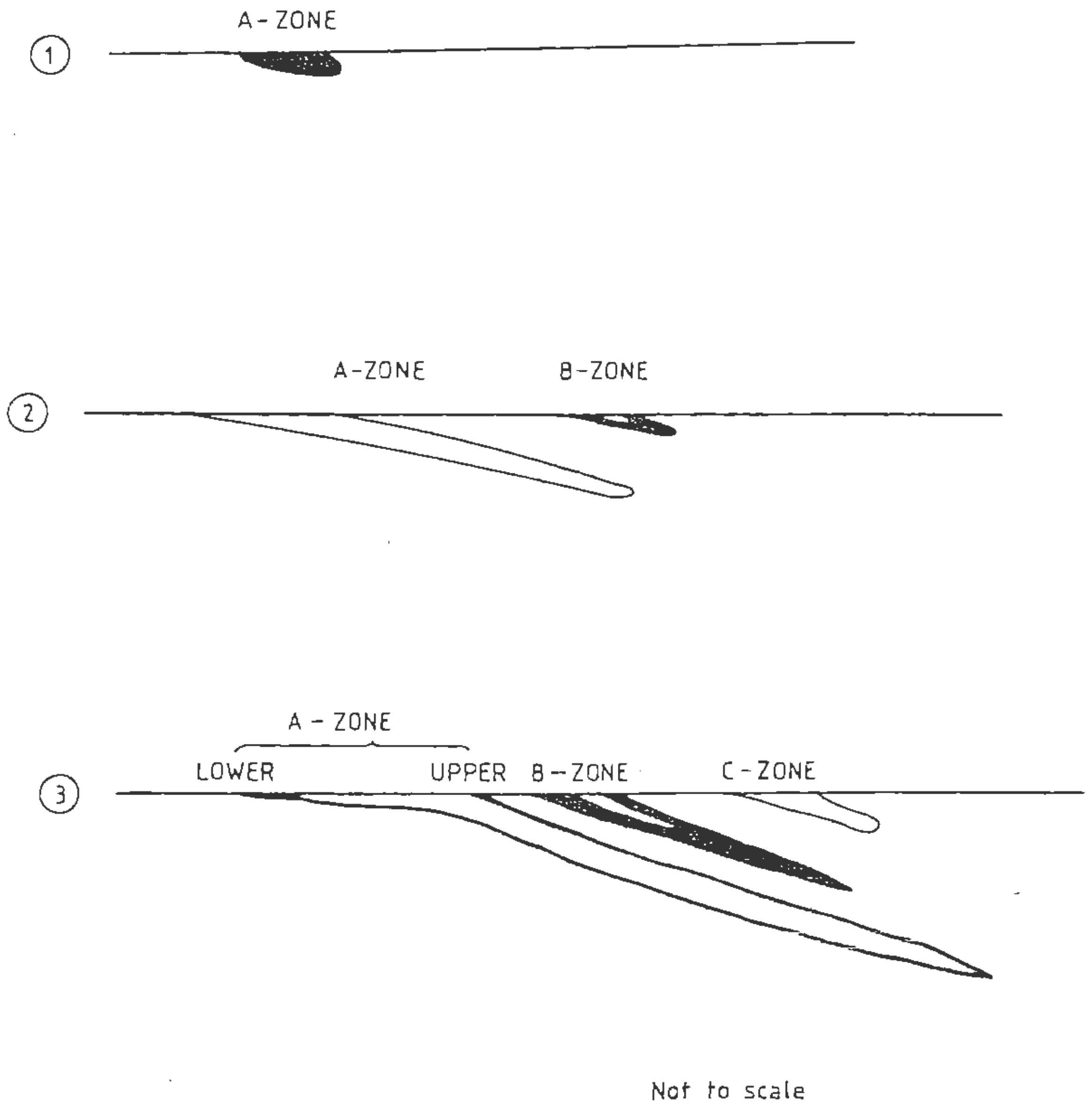

Fig 12 Simplified sections to illustrate the structural interpretation of the orebodies at Moonlight (See fig 11 for the positions of section lines)

Although no major displacement of the MEQ-orebodies was found, fault gouge, cataclasite (up to 6 m thick), and even thin mylonite zones were intersected in drill-core (Plate 13). Due to the wide spacing and limited depth of boreholes, none of these structures could be correlated between the boreholes. They appear to be related to relatively late-stage deformation.

Plate 13 Cataclasite from the Moonlight project-area

Boudinage was found in some instances, but it is accepted that a lot of the small-scale structures were destroyed during subsequent deformation and metamorphism.

The majority of the faults observed in drill-core strike east-northeast and dip steeply at ±70° to the north, and they seem to have controlled the deposition of the Karoo rocks. Pegmatite veins are often associated with these faults.

On a regional scale, north-west-trending late-stage faults occur with north-west to northerly trends and could have produced the weak zones for diabase intrusion (the north-west-trending diabase at Moonlight?). Most of these trends may have been reactivated in post-Karoo times. Although no major displacement of the orebodies are shown on map and on the geological sections, more detailed drilling may change the interpretation when the fault structures can be correlated and interpreted on a smaller scale. Displacement along fault planes may then in places replace or modify interpreted fold structures.

5.2 METAMORPHISM

No in-depth study of the petrology and metamorphism of the Moonlight lithologies was carried out, and no conclusive time sequence of the different metamorphic events can thus be given. In spite of this the different events will be fitted into the regional tectonic framework of the Limpopo Belt as described by Van Reenen and Roering (1990), Horrocks (1981) and Watkeys et al (1983).

Two main metamorphic processes can be recognized at Moonlight viz a prograde metamorphic event giving rise to granulite-phase mineral assemblages (sillimanite+ almandite+orthopyroxene+quartz) overprinting the main fabric (foliation), and retrograde metamorphism which is seen in the chloritization of hornblende and biotite, sericitization of feldspars in metapelites and the serpentinization of olivine and pyroxene, especially in the ultramafic complexes. Amphibolites in the project-area may also indicate a retrograde event.

Figure 13 depicts the broad schematic metamorphic field as interpreted for the prograde metamorphic event (M1) at Moonlight.

The field depicted in figure 13 is defined on the basis of the following parameters:

1. The sillimanite+almandite+orthopyroxene+quartz paragenesis seen at Moonlight, indicate granulite phase metamorphism.

2. The absence of muscovite indicates that the following reaction took place:

   Muscovite + SiO_2 = K-feldspar + Al_2SiO_5 + H_2O.

3. Almandite in metapelites especially those with a high pyrope-content is present within the high-grade metamorphic field (from 5 kb pressure up). The isograd-line is still dependent on P-T conditions and the Mg/Fe-relationship.

4. Mainly sillimanite is found as Al_2SiO_5 in the Moonlight lithologies, which makes the andalusite-kianite-sillimanite stability curve applicable in the definition of a metamorphic grade.

Large scale serpentinization, with subsequent carbonitization and epidotization is recognized, especially in the ultramafic complexes. Epidotization can be seen to have replaced the feldspars in the gneisses, outwards from joints and fractures. Poikiloblastic tremolite-actinolite is also seen as a retrogressive product of diopside crystals.

Although the time sequence of most of these retrograde processes can be interpreted from core drilled in the project-area, they can still not be related to specific periods in time. The datings for chloritization, serpentinization and epidotization as given in table 4, are

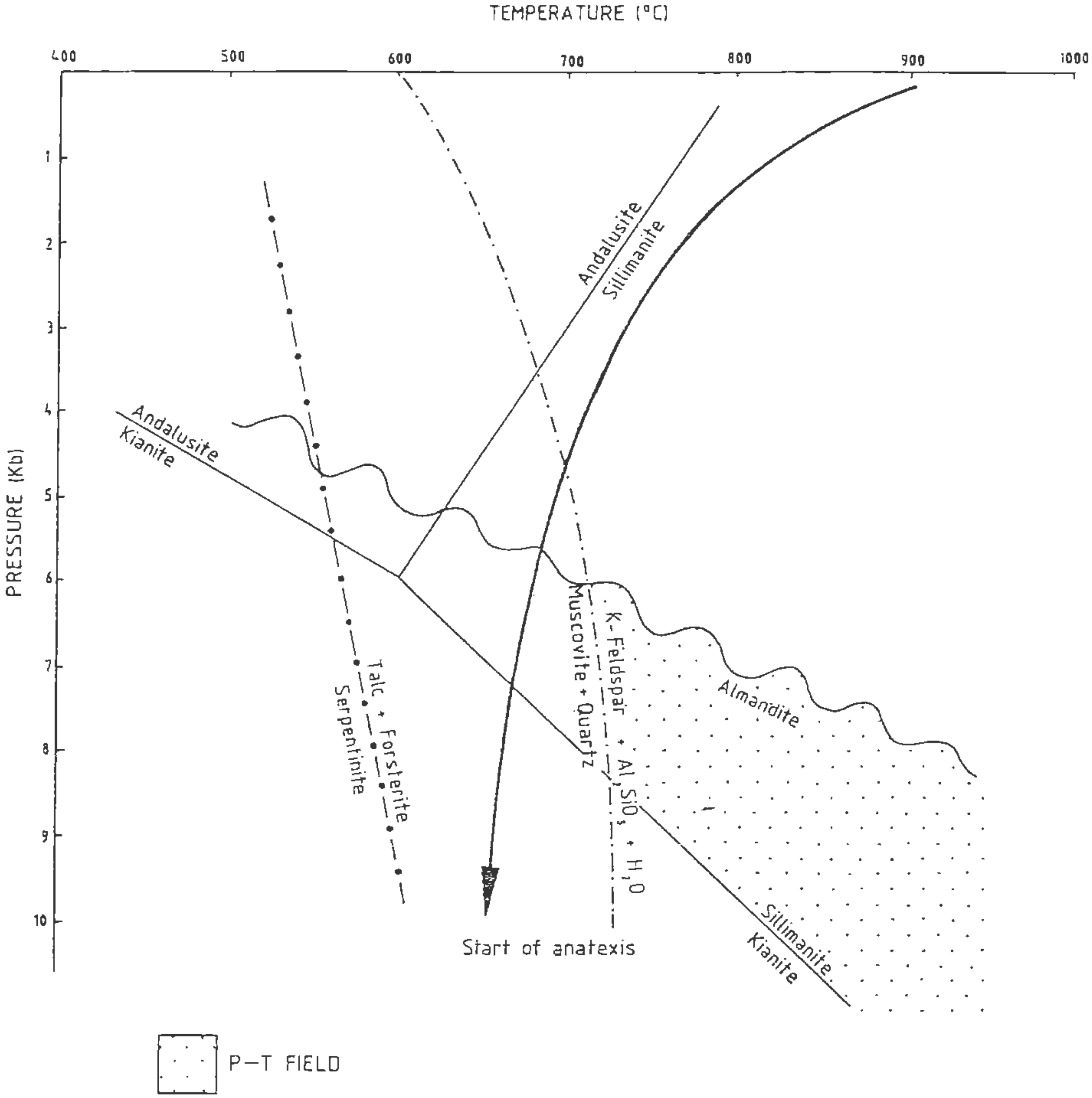

Fig 13 Temperature and pressure fields in the Central Zone of the Limpopo Belt during the period 3300Ma to 2600Ma as recognized from lithologies at Moonlight IIILR

therefore subject to change, but they appear to be younger than the process of sericitization seen in most of the feldspars. Two or more retrogressive metamorphic-phases are thus recognized. The retrogressive metamorphism is related to uplift, isothermal decompression and cooling after the main deformation phase (D1), of the Limpopo Orogeny, as described under 5.3.

The amphibolites associated with mafic granulites, which are present at Moonlight, represent amphibolite-facies metamorphism, but it is difficult to determine whether or not they represent the retrograde equivalents of previous granulites, or a prograde event.

More information applicable to the metamorphism of rocks from the Limpopo Belt, is given under section 5.3.

5.3 TECTONIC EVOLUTION OF THE LIMPOPO BELT

It is attempted in this section to place the Moonlight lithologies and their evolution in the broader perspective of the Limpopo Belt as a whole. It falls outside the scope of this project to discuss in detail the geological, geophysical and geochronological studies conducted on the Limpopo Belt and adjacent granite-greenstone terrains, but the most important constraints on the evolution of the Limpopo Belt will be mentioned.

From the work of authors like Horrocks (1981) and Watkeys et al (1983) it is known that before about 2800 Ma ago, more than one deformational event influenced lithologies of the Zimbabwe, Kaapvaal and Central Zone Cratons. These events are not discussed because they are not recognized at Moonlight. More emphasis is placed on the Limpopo Orogeny and subsequent events.

We do know for certain from Moonlight mineral assemblages that the Limpopo Belt lithologies were subjected to granulite-facies metamorphism at great crustal depths (at least 35 km), and that retrograde metamorphism occurred at a later stage, probably during uplift and decompression. Van Reenen and Roering (1990) discuss these points in detail, and some of their findings are listed below:

1. The highly attenuated nature of the supracrustal assemblages in granitoid gneisses resembles brecciation on a regional scale. The complex folding of these attenuated fragments and the development of macro-sheath folds suggests that simple shear has been the dominant deformational mechanism at great crustal depths.

2. The different tectonic terrains of the Limpopo Belt are all bounded by major shear zones up to several kms wide, which together with smaller shear zones, also separate domains of different metamorphic grade. Although it is believed that the majority of them originated during the Limpopo orogeny, some do display long complex histories of reactivation as recently as in Karoo times.

3. The orientation of movement vectors in the Southern Marginal Zone (SMZ), Central Zone (CZ) and northern boundary of the Kaapvaal Craton are all in a south-west, north-east direction, and the marginal zones are thrusted over the Rhodesian and Kaapvaal cratons.

4. Gravity, geoelectrical and seismic surveys are all interpreted by means of thrust-sheets indicative of continental collision (fig 14).

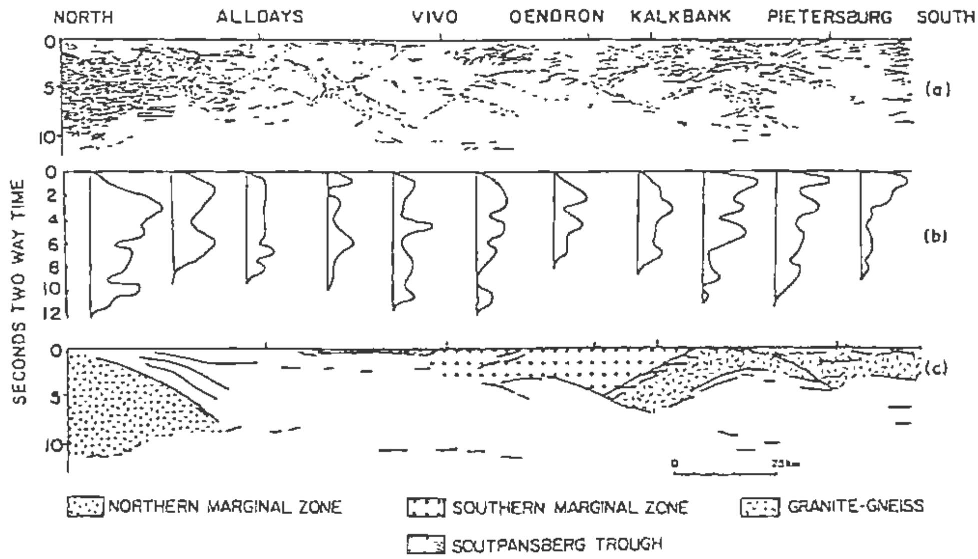

Fig 14 Results of a vibroseis survey conducted from Pontdrift in the north to Pietersburg in the south (Van Reenen and Roering, 1990)
(a) line drawing of the seismic record marking the most obvious linear reflectors (b) a plot of the amount of reflection times reflection length against depth in TWT (c) preliminary geological interpretation also taking into account the gravity and deep electrical sounding models

5. Rocks throughout the Limpopo Belt are characterized by two or more of the following features: (i) granulite-facies mineralogy (SMZ, CZ and NMZ); (ii) polymetamorphic granulite-facies (CZ and SMZ); (iii) mixed granulite and amphibolite facies (mainly CZ), and (iv) retrogressed equivalents of previous granulite-facies rocks (CZ, SMZ and NMZ).

6. Peak metamorphic conditions (M1) throughout the Limpopo orogeny is believed to have been in

excess of at least 7,5 kbar and 800-850° C, although evidence for peak metamorphic conditions during the prograde stage has almost been completely obliterated by the subsequent retrograde events. Peak pressure estimates of at least 9,5 kbar in the CZ are supported by the rare presence of relict kyanite being replaced by fibro-litic sillimanite (Watkeys et al, 1983). Pressures of between 8 and 9 kbar are interpreted for the SMZ, from the presence of prograde sillimanite in anatectic leucosomes associated with metapelite.

7. The M1-metamorphic event clearly postdates the main fabric-forming event, therefore suggesting that stable granulite conditions were superimposed on the main fabric (D1).

8. Isothermal decompression (M2) in the SMZ and CZ took place under essentially static conditions as indicated by the replacement of garnet and quartz by a symplectitic intergrowth of cordierite and unorientated second generation worm-like hypersthene in metapelite. Metapelites throughout the CZ are also characterized by various other decompression textures, which involve the replacement of garnet by hypersthene and plagioclase, garnet-sillimanite-quartz by cordierite, and biotite-sillimanite-quartz by cordierite and K-feldspar. Temperatures during this decompression event were greater than 750° C, while pressures were in the region of about 6 to 7 kbar (fig 15).

9. Decompression throughout the Limpopo Belt was followed by cooling and retrogression (M3) during the introduction of a fluid phase into the high-

grade lithology. This event established the retrograde orthoamphibole isograd in the SMZ, mappable zones of retrogression in both the SMZ and CZ, as well as local retrogression throughout most of the Limpopo Belt. Evidence for this local retrogression throughout the granulite zones of the Limpopo Belt is suggested by numerous retrograde reactions, involving mainly the replacement of pyroxene by hornblende in mafic granulites, and of hypersthene by biotite in pelitic granulites. Isogradic P-T conditions were between 600°C - 625°C, and pressures between 5 and 6 kbar (fig 15).

10. An important aspect of the metamorphic evolution of the Limpopo Belt is its uniform grade of metamorphism (fig 15), eg the present (M2) pressure gradients are small (± 2kbar), ranging between 6 and 8 kbar over distances of up to 200 km. This indicates that no intercalations of higher and lower-grade rocks exist which can be interpreted as tectonic stacking.

11. The clockwise P-T-time evolution of the CZ, SMZ and NMZ (fig 15) records a single continuous loop and implies that heating occurred only after tectonic loading.

12. The CZ are regarded as having been a separate crustal segment, because it appears to have distinctive shelf-type and Messina Suite lithologies, whereas the marginal zones are modified equivalents of granite-greenstone material.

13. The post-peak hydrating fluid was CO_2-rich at a wide range of P-T conditions.

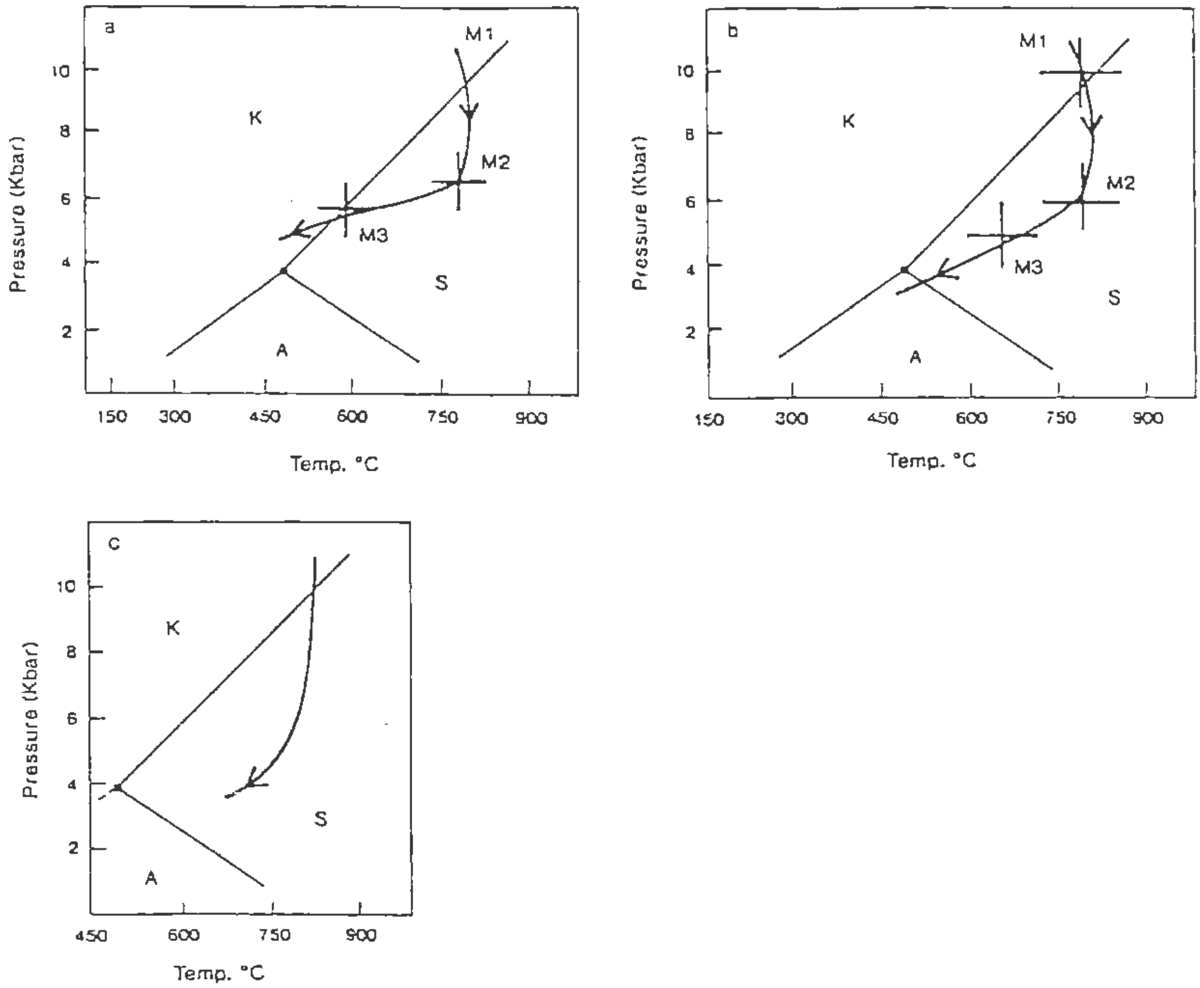

<u>Fig 15</u> P-T trajectories for the granulites from the Limpopo Belt (a) for the SMZ; (B) for the CZ near Messina; and (c) after Windley, et al 1984 (Van Reenen and Roering, 1990)

From the information listed above, a picture of the evolution of the Limpopo Belt is starting to form, but the timing of the different events is still problematic. Barton (different references) did most of the radioactive isotopic dating, with additional input by other workers eg Harris et al (1987). Despite years of research in this field, at present only four time points in the tectonic evolution of the rocks exposed in the Limpopo Belt and the adjacent Kaapvaal and Zimbabwe cratons have been precisely defined (Barton, in Van Reenen and Roering, 1990).

1. The emplacement of granitic and granodioritic plutons and granitic pegmatite throughout the CZ, SMZ and adjacent Kaapvaal Craton, between about 2700 Ma and 2650 Ma ago.

2. The formation of charnockitic rocks geographically associated with the Matok Pluton sometime between 2673 Ma and 2667 Ma ago (Part of the Limpopo Orogeny?).

3. The emplacement of the Bushveld and Palabora Complexes between 2070 Ma to 2050 Ma ago.

4. The cooling of rocks on a regional scale below the blocking temperature of biotite in the Rb-Sr and K-Ar systems between approximately 2100 Ma and 1950 Ma, due to uplift and erosion.

The interpretations of all other isotopic ages, of which there are many tens, is ambiguous and in most instances, it has not been possible to substantiate any of these ages by using alternative isotopic techniques (Barton, in Van Reenen and Roering, 1990). Answers as to when most of the various lithologies were emplaced, when the tectonic events affecting them occurred and when metamorphic conditions were reached during the Limpopo Orogeny as yet cannot be answered except in very general terms.

According to Van Reenen and Roering (1990), Pb-isotopic compositions of lithologies 2690 Ma or older in the CZ are much more radiogenic than those from the SMZ and Transitional Zones, implying that the lithologies of the CZ evolved independently of those in the SMZ and adjacent portions of the Kaapvaal Craton before about 2690 Ma.

From the evidence available it thus seems as if the Limpopo Orogeny occurred between about 2700 Ma and 2650 Ma. Metamorphism and deformation associated with the Limpopo Orogeny in the NMZ was also completed by the time of emplacement of the Satelite Dykes to the Great Dyke Complex about 2545 Ma ago (Van Reenen and Roering, 1990).

The most important time points in the evolution of the CZ, SMZ and the adjacent portion of the Kaapvaal Craton are outlined in table 4, including the events seen at Moonlight.

A continental collision-model thus seems apparent, and the presence of three different cratons implies some sort of accretionary setting. It is difficult to explain what happened to the oceanic crust involved, although some of the ultramafic complexes may be regarded as being ophiolites.

Different models were published by Coward (1983), Light (1982), Van Reenen et al (1987), and Van Reenen and Roering, and McCourt and Vearncombe, in Van Reenen and Roering (1990). Three main interpretations of collision geometry exist, viz north-west-south-east collision with the Kaapvaal Craton overriding the Zimbabwe Craton, north-south (north-east-south-west) collison of the Kaapvaal and Zimbabwe cratons with the CZ-craton caught-up in between, and east-west collision of the CZ-craton with the already joined Zimbabwe and Kaapvaal craton.

Although the east-west collisional model satify the structural analysis on most of the major shearzones bounding the CZ, these vectors are regarded as the product of later stage reactivation of the shearzones, and the D1-movement vectors within the CZ as well as lineations at Moonlight are oblique to the proposed movement direction.

Table 4 Important time-points in the evolution of the rocks comprising the CZ, SMZ and the adjacent portion of the Kaapvaal Craton (Modified after Van Reenen and Roering, 1990)

Sedimentary and igneous events		Time (Ma)			Products	Seen at Moonlight
						Sand, calcrete, ferricrete
Mafic dykes	▪▪	180		M5	Contact metamorphism	Post Karoo faults and joints
Nuanetsi Ign Prov	▪▪	190	D6			Epidotization ?
Karoo	▪▪	300				Karoo sediments
	▪▪	400				
Kimberlite	▪▪	700				
	▪▪	1200				
	▪▪	700				
Mafic dykes	▪▪	1250				Diabase dykes
	▪▪	1500			Folding and faulting of	
Waterberg		1800	D5		Waterberg rocks	
Mafic dykes▪▪ Entebeni	**	1900				
Rb-Sr	**	1950			Mylonitized rocks of the	Mylonite
Biotite ages	**	2000	D4		Bushveld Complex	
Bushveld, Schiel	**	2050				
+ Palabora Complexes	**	2100				
Mafic dykes	▪▪	2200		M4	Steep mylonite zones	Mylonite
			D3		Flat-lying cataclastic zones	Cataclasite
Palmietfontein granite	▪▪	2450			Folding with diapiric uprise	Interference fold structures
Great Dyke	**	2500	D2		Folding and ductile shearzones	Chlorite, serpentine, carbonate
Lamprophyric dykes	▪▪	2600		M3	Orthoamphibole isograd	Amphibolite assemblages
				M2	Decompression textures	
Granodioritic and					Pegmatite	
granitic plutons	**			M1	Charnokite	
LIMPOPO OROGENY	▪▪	2700	D1		Granulite	Granulite assemblages
Alldays gneiss	++				Recumbant and isoclinal folding	Isoclinal folds and L1-lineation
Duiwelskloof pluton	▪▪	2800				
Goudplaats gneiss	▪▪	2880				
Mafic dykes and						
Klein Letaba gneiss	▪▪	3000				
Messina Suite	++	3150				Ultramafic Complexes
CZ-supracrustals						Supracrustal rocks
Sand River Gneiss	++	3300	D0		Deformed basement gneisses	
Baviaanskloof Gneiss						
Eersteling Formation	++	3450				
(greenstones)						

** well known ▪▪ probable ++ minimum estimate

More detailed structural analyses over the whole of the Limpopo Belt and adjacent Cratons is needed before the geotectonic model can be satisfactorily resolved, but the following simplified model is proposed based on the information available (fig 16).

Stage 1: North to north-west directed thrusting of the CZ-craton onto the Zimbabwe Craton, creating the main movement directions in the NMZ and along the Tuli-Sabi Shearzone.

Stage 2: Collision of the Kaapvaal Craton with the CZ and Zimbabwe Cratons in a north-east, south-westerly direction just after but superimposed on initial collision in Stage 1. This north-east directed collision (D1) led to crustal thickening, tectonic loading, reorientation of most existing structures and subsequent granulite formation. Thrusting of the high-grade Limpopo lithologies onto the adjacent cratons also took place during this D1-event. High-angle reverse faults as described by Van Reenen and Roering (1990) formed due to the unstable thickened crust that formed.

Stage 3: Thermal readjustment took place which led to the M2-metamorphic event.

Stage 4: Isostatic readjustment took place through erosion of the mountain-belt and subsequent decompression. This decompression was followed by cooling and retrogression (M3).

Later reactivation of the main boundary shearzones which was not part of the Limpopo Orogeny, enhanced and straightened them although in a more lateral orientation. These later tectonic movements created the interference folding, shearing and cataclasite and mylonite zones, seen at Moonlight.

In this model it is taken into account that the granite-greenstone terrains of the Kaapvaal and Zimbabwe cratons were already formed before the Limpopo Orogeny. Earlier deformational events therefore took place, also in the CZ-craton (Watkeys et al, 1983 and Horrocks, 1981), before the D1-deformation of the Limpopo Orogeny (table 4).

6. ECONOMIC AND MINING ASPECTS PERTAINING TO THE MOONLIGHT MAGNETITE QUARTZITES

6.1 GEOMETRY AND STRUCTURE

The magnetite quartzites at Moonlight underlie an area of 2,6 km^2 and vary in depth from surface to at least 450 m in the northern part of the project-area (Maps 1, 2 and 3 in back pocket).

The strike of the magnetite quartzite orebodies is generally 070° with dips of 6° and 18° to the north in the southern and northern parts of the project-area respectively.

The orebody is divided into different ore-zones/bodies for interpretation purposes, with the A-ore zone stratigraphically the lowermost/deepest (fig 5 and Map 4). It is important to note that the different ore-zones do not consist of only magnetite quartzite, but that numerous interlayered waste (gneiss, granulite) and intrusive rocks do occur. The character of the ore-zones also differs from borehole to borehole, which makes ore/waste ratio interpretation in undrilled positions difficult. Only the broader ore-zones (Lower A, Upper A, B and C) can be correlated between the different boreholes, due to the variable character of the ore-zones (see table 5).

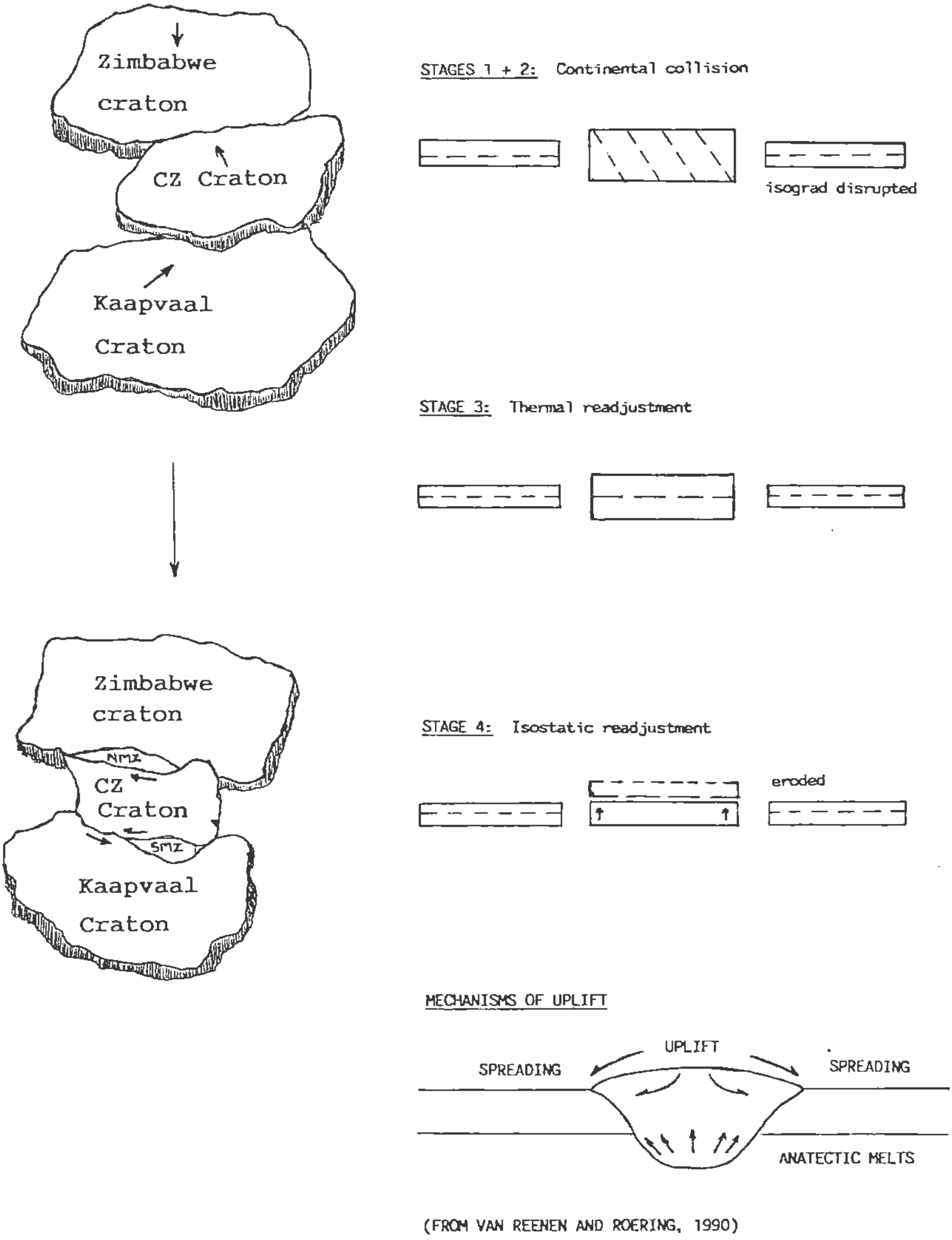

Fig 16 Simplified geotectonic model for the evolution of the Limpopo Belt

Table 5: **Borehole intersections of the A and B ore-zones illustrating the variability in thickness of the ore-zones and the associated internal waste.**

Borehole No	Orezone	Thickness (m)	Thickness of internal waste (m)
Mt9	A	6,72	0,00
Mt13	A	51,39	8,10
Mt31	B	52,28	0,00
Mt35	A	82,41	16,12
Mt63	A	28,52	14,07
Mt64	A	15,57	0,00
Mt34B	A	139,51	69,52

Figure 11 and the geological sections given in Map 3 in the back pocket seen together, show the structure and geometry of the Moonlight ore-zones in a 3-dimensional perspective. It will only be possible to get an accurate interpretation of the structure of the orebodies when a drill-grid of at least 100 m x 100 m has been drilled. At this stage it can only be said that the magnetite-ore occurs in three zones that may be the product of isoclinal folding of a single iron-formation-deposit. The upper part of the tilted sequence was subsequently eroded, leaving only the bottom half of the deposit intact, which is at present represented by the A, B and C fold-closures (fig 12).

6.2 MINERALOGY

The magnetite quartzite is dark-grey to black in colour, medium to coarse grained, with a granoblastic tecture. Quartz, magnetite and hematite are the main constituents which occur in variable amounts: quartz (20-64%); magnetite (5-58%) and hematite (0-49%)

Magnetite ($Fe_2O_3.FeO$) is found as aggregates, anhedral rounded crystals and as euhedral crystals which vary in size from 40 µ to 3 mm.

Hematite (Fe_2O_3) is present as fine lath-like intergrowths in the magnetite crystals, parallel to the octahedral planes and as oxidation product of magnetite in the weathered zone. It may also be found as irregularly-rounded grains, aggregates or as pseudomorph of magnetite where full martitization took place close to the surface, or sporadically as a primary mineral or metamorphic product in depth.

From borehole information, it is known that the lithologies at Moonlight are weathered up to 50 m depth. This implies that most of the ore-zone has been relatively oxidized to this depth, through the following process.

Magnetite+oxygen = maghemite(magnetic)+oxygen = hematite

$4Fe_2O_3.FeO+O_2 = 6Fe_2O_3$

Drill-core samples were mineralogically investigated in order to determine the magnetite and hematite contents. This is necessary as the oxidation-state of the ore can have a negative influence on recoveries during beneficiation.

Figure 17 illustrates the variation in magnetite/hematite content of the orebodies with depth from surface. Down to a depth of 40 m, magnetite and hematite occur in roughly equal amounts, but with hematite a little more abundant. At greater depths it is obvious that magnetite is the dominant ore-mineral, although hematite may be dominant in a few samples, probably due to oxidation along fault planes. Table 6 shows the distribution of magnetite and hematite in selected boreholes.

TABLE 6 Distribution of magnetite and hematite in selected boreholes

Borehole	Zone	Ore intersection		% Magnetite in intersection	% Hematite in intersection
		From	To		
MT51	A	220,45	236,21	100,00	0,00
MT2	A	12,00	26,28	41,70	58,30
MT35	A	145,08	227,49	100,00	0,00
MT15AD	B	2,00	37,06	20,10	79,90
MT31	B	78,68	130,96	98,30	1,70
MT51	B	152,62	205,70	94,50	5,50
MT33	C	20,00	58,69	32,80	67,20

Trace amounts of **goethite** ($HFeO_2$) and limonite ($HFeO_2.nH_2O$)(<1%) are found as residual weathering products of magnetite.

Quartz (SiO_2) is the main gangue mineral and occurs as xenoblastic and irregular lengthened grains, which are in general coarser-grained than the magnetite.

Amphiboles occur in subordinate (<5%) to trace amounts, and comprise actinolite ($Ca_2(Mg,Fe)_5Si_8O_{22}(OH)_2$), **hornblende** ($Ca_2Na(Mg,Fe^3,Fe^2,Al)5Si_6Al_2O_{22}(OH,F)_2$) and probably **hastingsite** ($((Ca_2,Na+K)(Fe^2,Mg)_4Fe^3Si_6Al_2O_{22}(OH)_2$).

Plagioclase ($Ca_2Al_2Si_2O_8$ - $NaAlSi_3O_8$) and **K-feldspar** ($KAlSi_3O_8$) are found in subordinate amounts (<5%).

Talc ($Mg_3(Si_2O_5)_2(OH)_2$), **chlorite** ($(MgFe^2,Fe^3+Al)_6(Si,Al)_4O_{10}(OH)_8$) and **calcite** ($CaCO_3$) generally occur in trace amounts (<1%), but may also be found in subordinate amounts (0-5%).

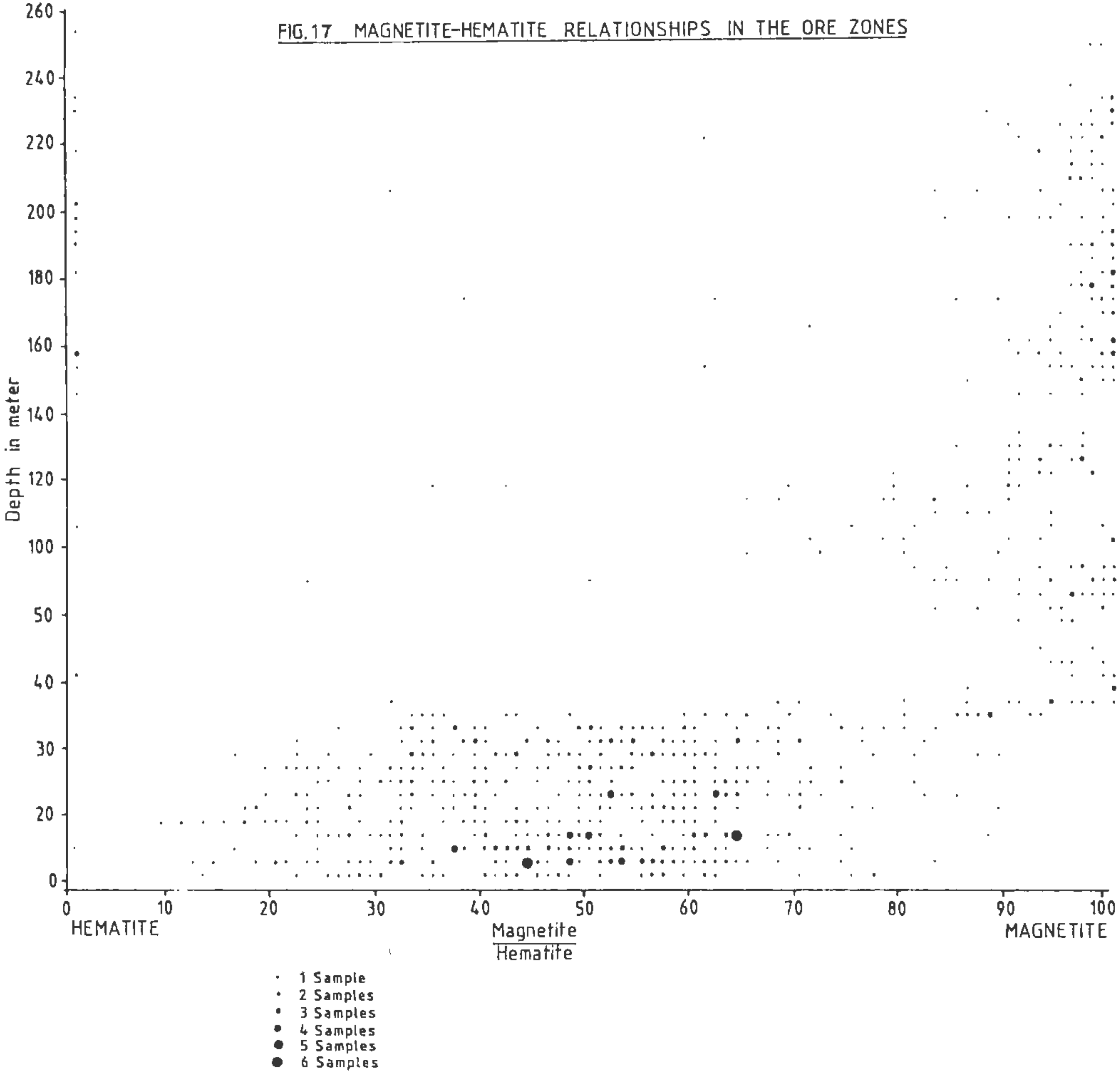

FIG.17 MAGNETITE-HEMATITE RELATIONSHIPS IN THE ORE ZONES

Other minerals that may occur in trace amounts include mica, garnet, epidote and clay minerals of the smectite-group (<1%).

Apatite, grunerite and titanite were found in a single borehole within the ore-zones (<1%).

6.3 CHEMISTRY

Seventy-two diamond drill-holes were drilled in the Moonlight project-area and chemical analyses were carried out on all of the ore-intersections. Combined results for the different ore-zones are shown in figure 9, while results on selected boreholes are given below in order to illustrate the change in chemistry with an increase in the amount of interbedded waste. Positions of all the boreholes are given on Map 1, in the back pocket.

A ore-zone

MT51

Ore intersection from 220,45 m to 236,21 m (15,76 m)
Thickness of ore alone = 12,07 m
Thickness of internal waste = 3,69 m
Average Fe-content of the ore-zone = 23% (internal waste included)
= 26,4% (internal waste excluded)
Average composition at ± 23% Fe (total iron)

Fe	SiO_2	Al_2O_3	K_2O	P	Mn	TiO_2	CaO	MgO	Cr_2O_3
23,21	57,81	3,27	0,12	0,061	0,02	0,11	0,31	3,65	0,02

Magnetite-content between 10% and 55%; average = 31,07%
Hematite-content between 0,1% and 12,3%; average = 1,18%

MT2

Ore intersection from 12,00 m to 26,38 m (14,38 m)
Thickness of ore alone = 13,18 m
Thickness of internal waste = 1,20 m
Average Fe-content of the ore-zone = 28% (internal waste included)
= 33% (internal waste excluded)

Average composition at ± 28% Fe

Fe	SiO_2	Al_2O_3	K_2O	P	Mn	TiO_2	CaO	MgO	Cr_2O_3
27,7	53,19	1,76	0,11	0,019	0,10	0,11	0,40	2,24	-

Magnetite-content between 8,4% and 30,1%; average = 18,9%
Hematite-content between 12,6% and 40,1%; average = 27,8%

MT35

Ore intersection from 145,08 m to 227,49 m (82,41 m)
Thickness of ore alone = 66,29 m
Thickness of internal waste = 16,12 m
Average Fe-content of the ore-zone = 30% (internal waste included)
= 34% (internal waste excluded)

Average composition at ±30% Fe

Fe	SiO_2	Al_2O_3	K_2O	P	Mn	TiO_2	CaO	MgO	Cr_2O_3
30,8	37,09	0,76	0,06	0,051	0,04	0,21	2,12	2,39	0,06

Magnetite-content between 21,5% and 55%; average = 43%
Hematite-content between 0,30% and 25%; average = 3,22%

B ore-zone

MT15AD

Ore intersection from 2,00 m to 37,06 m (35,06 m)
Thickness of ore alone = 35,06 m
Thickness of internal waste = 0,00 m
Average Fe-content of the ore-zone = 42,5%
Average composition at 42,5% Fe (total iron)

Fe	SiO_2	Al_2O_3	K_2O	P	Mn	TiO_2	CaO	MgO	Cr_2O_3
42,5	39,68	0,10	0,02	0,032	0,02	0,02	0,17	0,52	0,02

Magnetite-content between 9,9% and 36,1%; average 21,44%
Hematite-content between 19,5% and 53,6%; average 37,28%

MT31

Ore intersection from 78,68 m to 130,96 m (52,28 m)
Thickness of ore alone = 52,28 m
Thickness of internal waste = 0,00 m
Average Fe-content of the ore-zone = 38,13%
Average composition at 38,13% Fe

Fe	SiO_2	Al_2O_3	K_2O	P	Mn	TiO_2	CaO	MgO	Cr_2O_3
38,13	41,21	0,51	0,01	0,049	0,04	0,02	1,05	2,03	0,02

Magnetite-content between 29,4% and 57%; average = 44,8%
Hematite-content between 0,5% and 32%; average = 7,2%

C ore-zone

MT33

Ore intersection from 20,00 m to 58,69 m (38,69 m)
Thickness of ore alone = 20,78 m
Thickness of internal waste = 17,91 m
Average Fe-content of the ore-zone = 26,08% (including internal waste)
= 33,28% (excluding internal waste)

Average composition at ± 26% Fe (total iron)

Fe	SiO_2	Al_2O_3	K_2O	P	Mn	TiO_2	CaO	MgO	Cr_2O_3
26,08	44,81	3,53	0,16	0,065	0,14	0,41	5,56	5,56	0,03

Magnetite-content between 8,3% and 50,8%; average = 28,2%
Hematite-content between 1,4% and 37,4%; average = 15,1%

From the chemical compositions listed above, it can be seen that the ore all over the project-area is very similar regarding its chemical composition (excluding variability in total Fe and SiO_2), and that only the highly varying amounts of internal waste (mostly gneissic lithologies), influence the composition. It is also obvious that elements like K_2O and P, which could have a negative effect on steel produced from this ore, are present in negligible amounts, especially when it is taken into account that the ore is still to be beneficiated.

The maximum concentration of each of the different deleterious elements allowed in iron ore feed to the furnaces, and the negative effect of the different elements on steel produced from this ore, are summarized below:

ELEMENT	SPECIFICATION	EFFECT ON STEEL PRODUCED
P	0,05% max	cracking when worked + imperfections
S	0,05% max	makes steel brittle
K_2O	0,15% max	produces excessive slag in smelting process

The histograms in figure 9 and appendix 1 confirm that the deleterious elements are found in very small to omissible amounts in the Moonlight ores. It must be remembered that the histograms were drawn up for the magnetite quartzite ore-zones prior to beneficiation and with all interbedded waste included, and it was found that in general the majority of the deleterious elements report in the tailings of the beneficiated ores. Most of the interbedded waste (low Fe-populations in figures 9a and 9b) can be mined selectively, but their analyses were included in the data for the histograms, because of the size of the selective mining units being unknown at this stage. The large amounts of interbedded waste within the C ore-zone (fig 9d) renders this ore-zone economically unmineable, except for areas which can be mined on a selective basis while stripping waste from on top of the other ore-zones.

Cr_2O_3-distribution

More information regarding the distribution of Cr_2O_3 is given here, because at a certain stage it was thought that the Cr-content of the ore could prove to be problematic regarding mining and beneficiation. If the Cr_2O_3 concentration is too high in iron ore feed, problems arise in the production of soft steels. Unstable conditions may also result in liquids used during beneficiation (heavy medium) if Cr_2O_3-concentrations are too high. Regarding mining, complex relationships between the ore and lithologies containing the chromite can also hamper selective mining of the waste lithologies.

To illustrate the relationship between the Moonlight lithologies and Cr_2O_3 analized, analyses for borehole Mt33B are plotted in figure 20. If seen in context with the geology given in Map 3 and 4 in the back pocket, the distribution of Cr_2O_3 in the Moonlight lithologies is better understood.

Cr_2O_3 is found at Moonlight as follows:

1. In solid solution in the crystal structure of the magnetite and hematite and probably to a lesser extent in the silicate minerals. Magnetite quartzite samples with 15% or more total Fe, contain on average 0,06% Cr_2O_3 (calculated from 2193 samples). The mode is 0,02% which is negligible.

2. Sporadically in the internal waste (with less than 15% Fe) which would be mined with the magnetite quartzite. 104 Samples of waste associated with relatively high-grade ore, had an average Cr_2O_3-content of 0,26%, and 31 samples of waste associated with low-grade ore (15-19,99% Fe) had an average Cr_2O_3-content of 0,42%.

3. The highest concentrations of Cr_2O_3 are found as chromitite lenses in the ultramafic lithologies which are closely associated with the magnetite quartzite (fig 20 and map 4).

4. Sporadic values of between 1% and 2% Cr_2O_3 are found associated with amphibolites (fig 20).

The effect of the Cr_2O_3-distribution as described above, is as follows:

High Cr_2O_3-values are limited to the ultramafic lithologies which are closely associated with the magnetite quartzite, but are not that abundant at Moonlight. Most of the ultramafic lithologies present could be mined selectively and should not pose a problem during beneficiation. Thinner bands which could not be mined selectively can be taken out at an early stage by means of cobbing.

The Cr_2O_3-distribution in rocks from the project area will therefore pose no problem in the quality and suitability of the ores for iron and steel making.

6. ORE RESERVES

In calculating the ore reserves, the total orebody was divided into 4 parts (fig 18) viz a western block, eastern block, northern shallow block (<50 m) and a northern deep block (>50 m). Ore-reserves and qualities were determined for ore-zones as indicated in black on the sections of Map 3 (back pocket). These ore-zones include all the thin bands of internal waste which can not be mined selectively. The blank areas on the sections indicate internal and interlayered waste which can be mined selectively, and which was thus not included in ore-reserve calculations. These waste-zones were taken into account in determining stripping ratios. Ore-zones less than 3 m in thickness and those which are highly irregular such as most of the C ore-zone, were excluded from the ore-reserves.

North-south cross-sections were used in the calculation of ore reserves. Surface areas on the sections were determined by means of a planimeter. North-south and east-west sections were interpreted on 100 m spacing over the whole of the project-area, and cross-correlated, increasing the reliability of ore-reserve estimates.

In situ ore-reserves for the different ore-blocks are given in table 7.

SUBOUTCROP MAP OF THE MOONLIGHT OREBODIES WITH THE DIFFERENT ORE-BLOCKS INDICATED

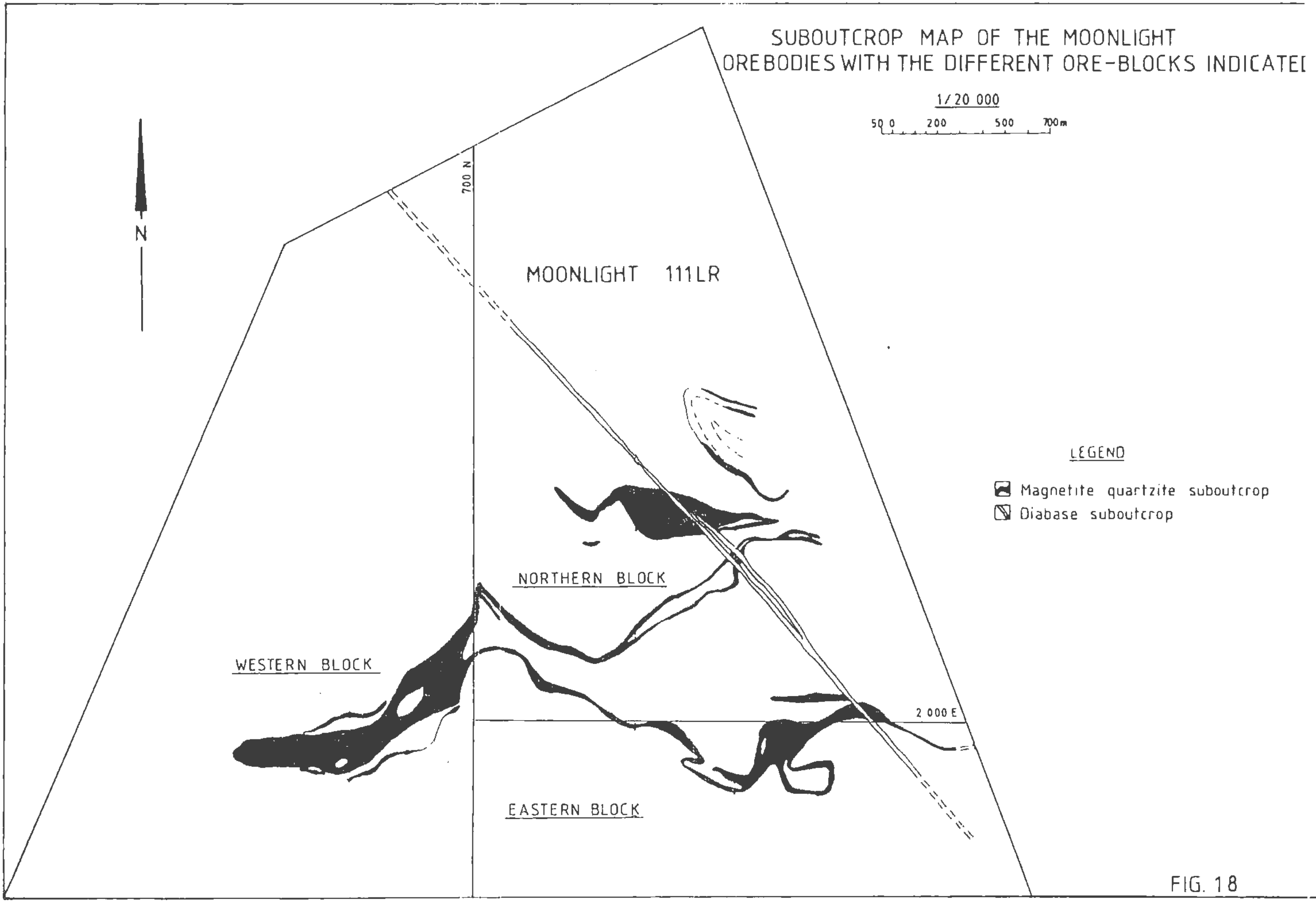

FIG. 18

Table 7 In situ ore reserves of the Moonlight project

Reserve Block	Ore reserves(Mt)	% Total Fe	RD *	% Magnetite	% Hematite	Mag/Hem
Western Block	10,2	33,65	3,38	21,04	27,78	0,76
Eastern Block	2,9	31,79	3,31	18,25	29,76	0,61
Northern Shallows	46,4	33,36	3,36	23,15	25,23	0,92
Northern Deeps	274,2	30,30	3,29	42,94	4,70	9,14
TOTAL	336,5	31,91	3,33	38,98	8,41	4,63

* RD = relative density

From the data in table 7 it is obvious that most of the ore reserves are present at depth (>50 m) neccessitating waste stripping. However, it was found that with a reasonable stripping ratio of 2,86:1 and a pit slope of 45° in the weathered zone and 55° in the unweathered rock, 287 Mt of ore can be mined to a pit depth of approximately 400 m. A mine-safety zone of 100 m along the farm boundaries has been taken into account in the calculation of mineable reserves. Extraction of additional underground reserves can be made from the open pit at a later stage, if economically viable.

6.5 BENEFICIATION

A range of beneficiation tests were conducted in conjunction with the Iscor Pilot Plant, in order to try to optimize the beneficiation of the Moonlight-ores. The main thrust of the investigation was to attempt to discard as much waste material as possible at a coarse size, thus reducing the volume of material to be further treated and upgraded. The tests conducted included the following:

1. Dry magnetic cobbing on oxidized and unoxidized ore (belt magnetic separation at a 5mm particle size)
2. Wet-drum magnetic separation on products obtained from the cobbing-stage

3. Hydro-separations, flotation and gravity tests
4. Mineralogical investigations and chemical analyses on the products obtained from 1, 2 and 3.

The following results were obtained from the beneficiation tests conducted:

1. Optimum liberation of the iron-oxides was obtained at a grain size of -150 μ
2. Both the oxidized and unoxidized ore can be beneficiated to an iron-ore concentrate with 69 - 70% Fe. An example product analyses is shown below:

Fe	SiO_2	Al_2O_3	K_2O	P	Mn	TiO_2	CaO	MgO	Cr_2O_3
69,20	2,86	0,35	0,02	0,010	0,05	0,02	0,21	0,22	0,05

3. With second and third-stage magnetic separations the unoxidized ore gave an iron recovery of 85-86% and a concentrate with a composition as above.

4. Magnetic separation on oxidized ore produced concentrate grades comparable to the unoxidized ore, but with slightly lower iron recoveries (± 81%)

5. Dry magnetic cobbing (at 5 mm) and table concentration (gravity) produced the best results in the first-stage beneficiation

6. Wet magnetic separation (-150 μ) resulted in the best results as a second-stage following the dry magnetic cobbing. A third stage wet magnetic separation may be used if necessary.

7. Flotation was mostly used in trying to upgrade the concentrate obtained from wet magnetic separation, and it produced reasonable grades but low recoveries.

8. The hydro-separation process improved the total Fe recovery in certain cases, but it had the effect of lowering the concentrate grade. This process is not recommended.

Although further tests are required in optimizing the beneficiation process, it can be seen from the results given, that a very good iron-ore concentrate can be produced with alkali, phosphorus and sulphur content within the specifications (section 6.3), excellent recoveries and with a relatively cheap beneficiation process (magnetic).

6. OTHER FACTORS THAT COULD INFLUENCE MINING

Quality distribution

Grades of the Moonlight orebodies vary significantly when interbedded waste is included. Taking only the magnetite quartzite without any interbedded waste into account, the percentage total Fe stays remarkably constant within the different orebodies as shown below (fig 9):

ORE-ZONE	% Fe (mode)
Lower A	38
Upper A	37
B	39

The higher grades and lesser amounts of interbedded waste of the B ore-zone (fig 19) could be used to advantage if part of it (up to 100 m depth?) is mined simultaneously with the stripping of waste overlying the deeper ores (A+B). This will give more flexibility in controlling the Fe-recoveries produced by the plant, and ensure a constant cash flow from an early stage of production.

Interbedded waste is common in the Moonlight ores (figures 9 and 19), and if incorporated in the ore to be mined, it results in low-grade zones in certain areas. In order to define these zones a distinction was made between ore (≥20% Fe), low-grade ore (15-19,99% Fe) and waste (<15% Fe). Due to the irregular character of the orebodies, these zones could not be correlated between the different boreholes. This means that to achieve proper grade control during a mining phase, a more detailed drilling program would be necessary and the information available from blast-holes would have to be incorporated.

Care should be taken during a mining stage, to mine the Cr-bearing lithologies (fig 20) on a selective basis as waste, to prevent chrome contamination of concentrates. In this regard, blending from areas of high and low chrome could also be useful.

Depth of ore

Most of the ore reserves at Moonlight are located at depth (Table 7) with the A ore-zone extending to 450 m below surface. This has a negative effect on open-cast striping-ratios and will require detailed studies on rock-stability and the most cost-effective mining methods and procedures, in optimizing the open-pit.

Rock-mechanical aspects

The flat-lying topography and thick sand-cover have resulted in a deep weathering profile; on average 50 m, but locally up to 70 m deep. With the exception of the magnetite quartzite, all the lithologies in the weathered zone would only require moderate blasting to break up. Most of the waste to be stripped will also be relatively easy to tear/rip, and this will keep stripping costs low. All unweathered rock and the magnetite quartzite in the weathered zone will require close spaced blasting in order to maintain excavation tempos.

FIGURE 19 MOONLIGHT PROJECT
Fe-values in samples from borehole MT33B

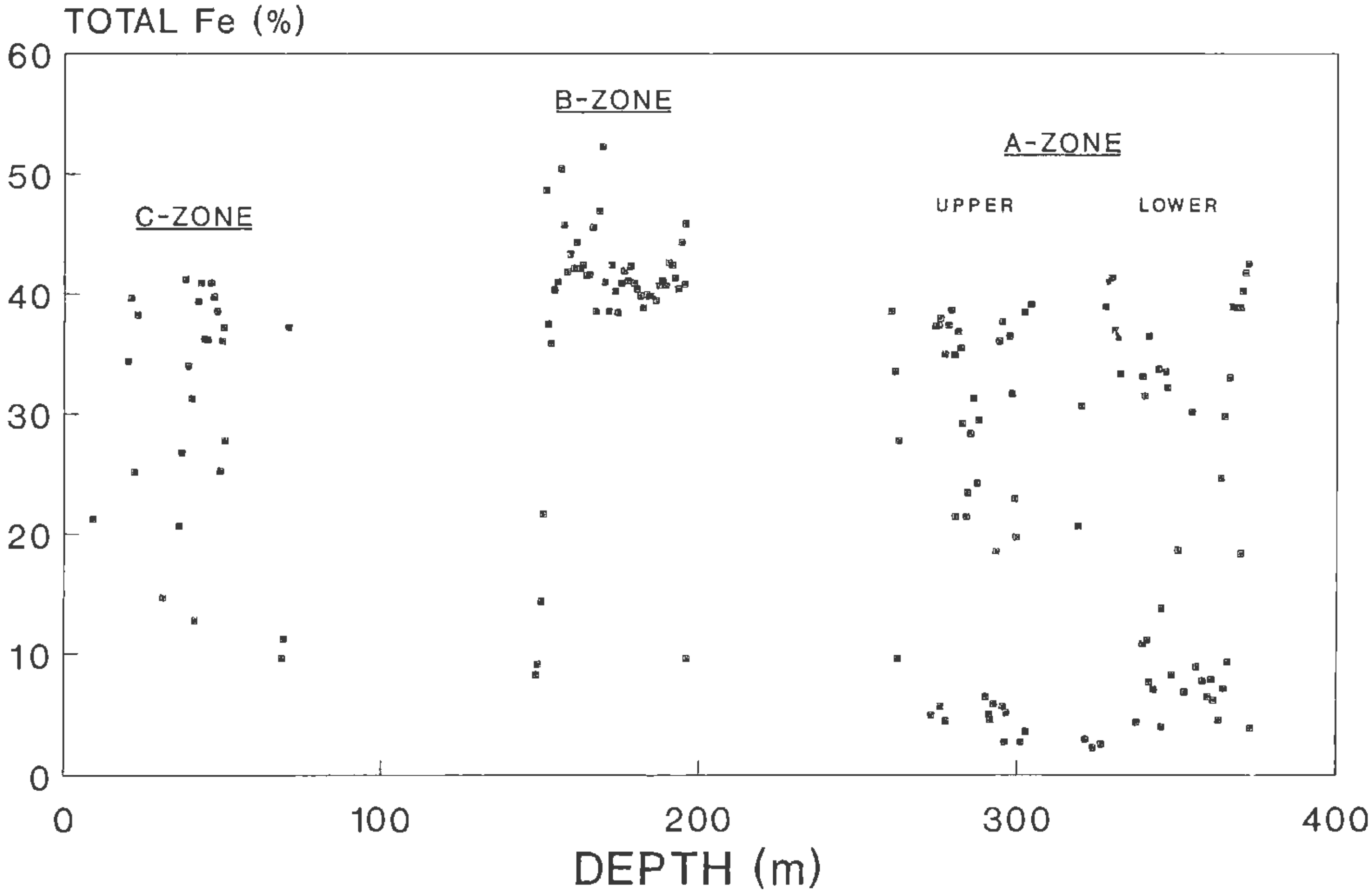

* WASTE SAMPLES WERE TAKEN ABOVE AND BELOW THE ORE ZONES
* SAMPLE INTERVALS ARE NOT ALWAYS THE SAME SIZE

FIGURE 20 MOONLIGHT PROJECT
Cr-distribution in borehole MT33B

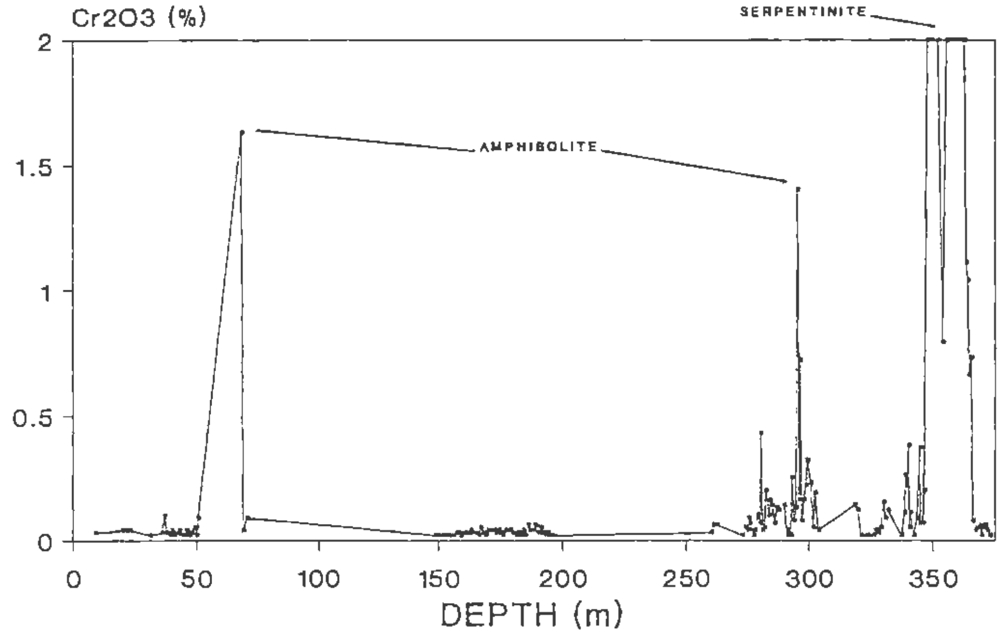

Cr-distribution in borehole MT33B

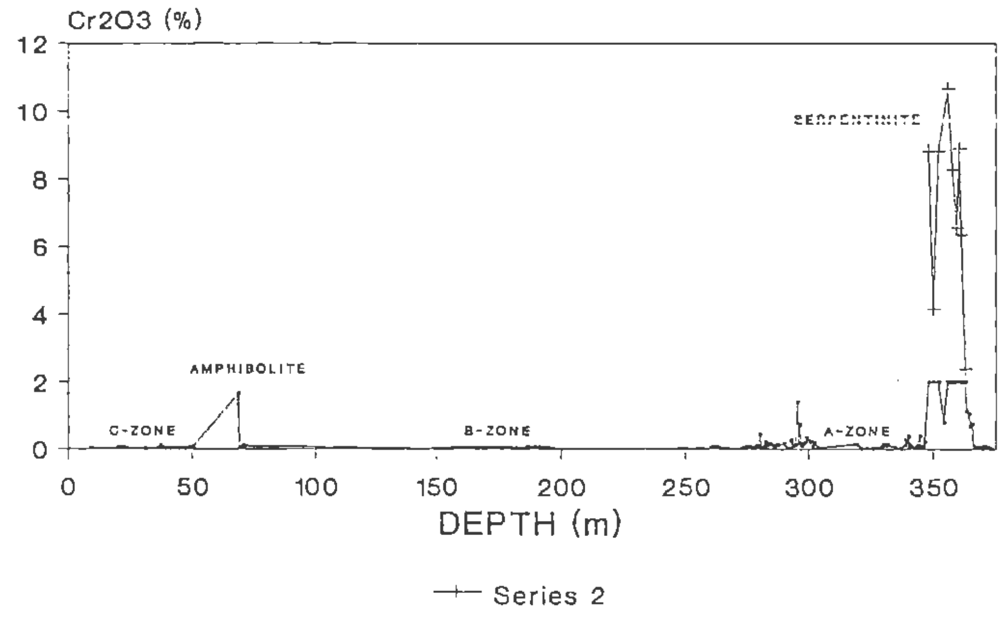

Drill-core from most of the boreholes was logged with respect to RQD (Rock quality designation), joint frequency, spacing, dips and fillings, and uniaxial compressive strength tests were carried out on selected drill-core samples (rock strength).

These results are summarized in table 8.

Structure

Polyphase deformation and high-grade metamorphism with associated remobilization of minerals, results in the orebodies being highly complex in geometry and structure. This should be taken into account in the exploitation thereof and mining should be well controlled. An estimate production phase drill grid spacing must be at least 50 m, with closer spacing (25 m) in problematic areas.

Although no large-scale displacement of the orebodies along fault-zones was recognized, displacements of up to 10m could have been missed, due to a lack of geological control (detailed drilling) and probably due to the complex and irregular structure of the orebodies masking displacement.

Intrusive rocks

Intrusive rocks may pose problems during the mining-phase as they may displace the orebodies or locally lower the grade. The pegmatites and the major diabase intrusive present at Moonlight can be mined selectively in most cases and thus not unduly influence ore-grades. The composition of the intrusives also are such that they would not pose any problems during beneficiation. The ultramafic lithologies present, may have high Cr_2O_3-contents, which could cause problems in the ore concentrate, but most of these bodies should be selectively mineable.

Table 8. Summary of the geomechanical properties of rock-units at Moonlight.

ROCK TYPE OR UNIT	ROCK STRENGTH (MPa)	RQD	JOINT FREQUENCY (j/m)	SPACING (m)	BIENIAWSKI CLASSIFICATION		*Blasting factor kg ANFO/m^3
					TOTAL VALUE	CLASS	
Highly weathered zone	15	12%	31	0,10 - 0,20	37	4	0,25
MEQ in weathered zone	89	71%	6	0,31 - 0,50	62	2	0,85
Weathered zone below MEQ	78	15%	30	0,10 - 0,21	42	3	0,37
Transition zone (to unweathered rock)	150 - 200	7%	33	0,09 - 0,20	55	3	0,36
Hornblende gneiss	156	73%	5	0,60	70	2	
Chlorite gneiss	150 - 200	64%	5	0,58	71	2	
Pegmatite	160	45%	10	0,23	52	3	
Granulite	253	66%	8	0,47	71	2	
Augengneiss	150 - 200	78%	4	0,59	75	2	
Garnet gneiss	150 - 200	61%	6	0,35	75	2	
Amphibolite	144	57%	8	0,54	55	3	
Biotite gneiss	184	58%	6	0,54	56	3	
Magnetite quartzite	232	78%	4	0,67	78	2	0,95 - 1,02
Average for all unweathered lithologies exclusive of the MEQ	194	67%	6	0,56	68	2	0,69 - 0,74

* Blasting factor : for weathered rock = $0,56\ RD\ \tan(\phi + i) / \sqrt[2\pi]{\text{frequency}}$

for unweathered rock = $0,56\ RD\ \sin(\phi + i) / \sqrt[2\pi]{\text{frequency}}$

* i = Angle of roughness

* ϕ = Basic friction angle

* RD = relative density

Water

The watertable in the Moonlight project-area is on average 35 m below surface. Percussion holes gave water yields of not more than 20 000 liter/hour and that only in selected spots. Underground water should therefore pose no threat to mining activities, on the contrary, water to be used for mining activities and beneficiation will have to be pumped from the nearest river or dam (for distances see section 1.2).

The quality of the water from the Moonlight aquifers is suitable for human consumption.

6.7 ECONOMICAL POTENTIAL OF THE MOONLIGHT OREBODIES

The Moonlight project and associated exploration was initiated on the basis of long term strategic planning, and was therefore not financially based on current metal prices. This makes it difficult to justify the project from a financial point of view, but an attempt is made in this section to evaluate the project in current money terms, mainly to evaluate the different options available in the exploitation of this deposit. No full-scale feasibility study was attempted for the Moonlight-project.

For the evaluation of a project, all factors that could have an influence on the project's cash flow or costs incurred, have to be taken into account. The most important cost factors for Moonlight which are at this stage relatively well known, are listed below:

Infrastructure

1. Railwayline	80 km
2. Tar road	30 km
3. Escom power	on site
4. Town (personnel)	80 km

5. Water (process)	30 - 50 km
6. Labour	12 km from own residences

Pre-production costs

1. Mineral rights	R 230 000
2. Exploration and evaluation	R 1 200 000
3. Follow-up exploration	R 2 000 000

Ore characteristics

1. Ore reserves (mineable)	287 Mt
2. Quality	32% total Fe
3. Stripping ratio	2,86 : 1
4. Beneficiation	Magnetic seperation
5. Quality of concentrate	69 - 70% Fe
6. Fe-recovery	± 83%

Production tempos will not be known before a market for the product has been established or before detailed feasibility studies have been completed. Two production alternatives viz 180000 tpm and 360000 tpm of magnetite concentrate were chosen for Moonlight, after taking the production of presently producing iron ore mines into account.

As for the production tonnages, a few other assumptions have to be made regarding mining and production:

1. Two products could be produced from the Moonlight ores after grinding down to -150μ for beneficiation. Magnetite fines as feed for direct reduction (DR) or pellets for DR or electric arc smelting. These products could be sold or used in local steelmaking.

2. Transport costs for export will be R 32-00/ton free on board (FOB) Europe, and R 12-00/ton to Pretoria.

3. Product prices will be R 38-00/ton and $ 20-00/ton for fines locally and FOB Europe respectively. If a pellitizing plant is errected, pellet prices will be R 120-00/ton locally and $ 65-00/ton FOB Europe. The exchange rate was taken as R 2-60 = $ 1-00.

4. The capital cost for a pellitizing plant with a capacity of 450 tph will be R 240 million, with the operating costs R 3,5 million and capital repayment R 3,7 million per month, while a plant with capacity of 900 tph will cost R326 million, with operating costs of R 7 million and capital repayment of R 5 million per month. All capital repayments will be made at a 18% interest rate over a period of 20 years, and are included under the costs given in table 9.

5. Capital and operating costs and capital repayment for the two alternative production rates and without a pelletizing plant will be:

Production rate (tpm)	Capital costs ($R \times 10^6$)	Operating costs per month ($R \times 10^6$)	Capital repayment per anum ($R \times 10^6$)
180 000	490	Mine = 4,45 Plant = 8,35	Mine = 20 Plant = 68
360 000	595	Mine = 8,90 Plant = 16,7	Mine = 107 Plant = 200

6. Mining costs will become progressively higher at higher stripping ratios as indicated below:

<u>Stripping ratio</u>	<u>R/ton mined</u>
0,5 : 1	R 2-80
1,0 : 1	R 5-00
1,5 : 1	R 6-10

2,5 : 1	R 9-00
3,0 : 1	R 9-40

At this stage it is still very risky to reach conclusions regarding the cash flows for the Moonlight-project, because of the many uncertainties surrrounding a possible mining venture. Besides the assumptions made above, one does not know for example what tax allowances will be applicable on such a mining venture, because these details are usually negotiated. It must also be stressed that low grade deposits like Moonlight may only become economically exploitable ore deposits in the long term.

Cash flows have been calculated for a 10 year period, for different mining and marketing options, and are included in appendix 2. Inflation, interest rates, price escalations and exchange rates were not taken into account, and no provision was made for replacement of mining or other equipment. Capital repayments are included in the costs (table 9). The results of the cash flow exercises are summarized below.

<u>Table 9</u> Summary of the results from cash flow studies for the Moonlight-project

FEED	PRODUCTION	CAPEX	FINE ORE			PELLETS			MARKET
	(tpm)	(R x 10^6)	COST (Rpm)	REVENUE (Rpm)	CASH FLOW (Rx10^6pa)	COST (Rpm)	REVENUE (Rpm)	CASH FLOW (Rx10^6pa)	
560 000	180 000	490 + 730	22,29 x 10^6	6,48 x 10^6	-189	29,47 x 10^6	21,60 x 10^6	-94	local
560 000	180 000	490 + 730	25,86 x 10^6	9,36 x 10^6	-198	33,10 x 10^6	30,42 x 10^6	-32	Europe
1 100 000	360 000	595 + 921	38,82 x 10^6	13,68 x 10^6	-302	51,02 x 10^6	43,20 x 10^6	-94	local
1 100 000	360 000	595 + 921	46,02 x 10^6	18,72 x 10^6	-328	58,22 x 10^6	60,84 x 10^6	31	Europe

* CAPEX = 110 + 350 = for fine ore + for pellets

* Transport costs are included under COST

It can be seen from the results obtained, that it will be very difficult to initiate an economic mining venture that only produces fine ore. The advantages of bigger production rates are confirmed with pellet production, and the product are obviously worth more in Europe than locally. To establish a secure market could however be a problem, and returns on local fine ore at lower production rates will be better than for fine ore sold in Europe. The cash flows and internal rate of return (IRR) for the Moonlight-project are obviously very sensitive to the product prices obtained and a better price could swing the profitability of the project very quickly towards positive cash flows. A very conservative dollar price was also taken for the iron ore pellets.

The cost of a pelletizing plant is very high, especially if the Moonlight returns on investment is taken into account. It must again be mentioned at this stage that the arguments put forward are not to justify a mining venture for Moonlight, but to emphasize the most critical factors which should be taken into account when the exploitation of the Moonlight ores is considered. In an economical climate where the Moonlight ores may be regarded as worth mining, the returns on a pellitizing plant may make it worth the investment. A further way in which the final returns of such a venture could be boosted is by using the pelletized product as direct feed in electric arc furnaces, and producing steel products. For Iscor pelletization and electric arc smelting looks to be the obvious route, especially if they can produce their own cheaper electricity from Grootegeluk coal.

The viability for the company to open up a mini-steelmill somewhere in north-western Transvaal is thus a project worth further consideration.

7. CONCLUSIONS

Magnetite quartzite is found in the Moonlight project-area, in association with a variety of paragneisses, granulites, other metasedimentary lithologies and ultramafic complexes. The magnetite quartzites were evaluated as potentially viable low-grade iron ore deposits by conducting an exploration program which included diamond drilling.

It was found that some of the magnetite quartzites extend from surface down to 450 m and are still open-ended in depth. All the lithologies were subjected to granulite-facies metamorphism during the Limpopo Orogeny, as well as to subsequent retrograde metamorphic events. This, together with complex folding which includes isoclinal folding, complicates the geometry and shape of the potential orebodies.

The magnetite quartzites present at Moonlight, represent 337 Mt in situ low-grade iron ore of which 287 Mt can be mined at a stripping ratio of 2,86:1. The mineable ore has an average total Fe content of 32% including interbedded waste. By using a two-stage magnetic separation beneficiation process, a magnetite-maghemite-hematite concentrate can be produced with a total Fe content of between 69% and 70%, and a Fe-recovery of approximately 83%.

Although the deposit is situated 350 km from the nearest steelworks at Pretoria, and its financial analysis gives a negative cash flow, it is regarded as a potentially viable ore deposit on the basis of the following points:

1. Moonlight is a large iron ore deposit with a relatively high magnetite content, a low content of deleterious impurities and it is relatively coarse-grained.

2. The Moonlight-area has good potential for dolomite, silica and to a lesser degree, limestone. These are some of the most important commodities used in the production of pig-iron.

3. Large reserves of coal are present in the Waterberg Coal Field, and coal is being mined at Grootegeluk Coal Mine at Ellisras, 80 km south of Moonlight.

4. With the commodities mentioned in 2 and 3 above, it may in future be a viable venture to open up a mini-steelmill in the Moonlight-Ellisras area. If this and some of the other recommended processes ie pellitizing and elecric arc furnaces, are taken into account, positive cash flows and a reasonable internal rate of return can be generated.

5. In addition to the Moonlight ore reserves, other low-grade iron ore deposits, although much smaller, are present in the Limpopo Belt.

6. High-grade iron ore deposits which are at present being exploited at mines like Thabazimbi and Sishen, may in future become exhausted or too expensive to mine and transport.

7. The lowest grade of magnetic taconite that is economically viable in the United States, has a minimum weight recovery of 20%. Moonlight-ores give recoveries of 40 to 55 weight percent.

Further follow-up exploration on the Moonlight orebodies should concentrate on the following:

1. More detailed diamond drilling (100x100 m grid) in order to get a better control on the structure and grade of the orebodies. Note should be taken of all structural features in drill-core eg breccias, cataclasite and mylonite, to try and determine the exact influence of these structures on the geometry of the orebodies.

2. Detailed metamorphic and petrological work on the full Moonlight lithological sequence in trying to establish a stratigraphical succession and/or structural sequence (eg tectonic stacking).

3. Detailed geohydrological study for the evaluation and utilization of groundwater for mining purposes.

4. Incorporation of all available information on a computer modelling program for 3-dimensional correlation, more accurate ore reserve calculations and geostatistical modelling.

5. Detailed feasibility study with incorporation of an open-pit design and beneficiation plant.

R E F E R E N C E S

Barton, J (1983a). Pb-isotopic evidence for the age of the Messina Layered Intrusion, Central Zone, Limpopo Mobile Belt. In : Van Biljon, W J and Legg, J H (Eds). The Limpopo Belt. Spec-Publ. Geol. Soc. S Afr, 8, 39-42.

Barton, J (1983b). Pb-isotopic studies of banded iron-formation, Central Zone, Limpopo Mobile Belt. In: Van Biljon, W J and Legg, J H (Eds). The Limpopo Belt. Spec-Publ. Geol. Soc. S. Afr, 8, 43-44.

Barton, J M, Fripp, R E P, Horrocks, P and Mclean, N (1979). The geology, age, and tectonic setting of the Messina Layered Intrusion, Limpopo Belt, southern Africa. Amer, J of Science, 279, 1108-1134.

Barton, J M and Key, R M (1983). Rb-Sr ages and geological setting of certain rock units from the Central Zone of the Limpopo Mobile Belt, near Zanzibar, eastern Botswana. In: Van Biljon, W J and Legg, J H (Eds). The Limpopo Belt. Spec-Publ. Geol. Soc. S. Afr., 8, 19-26.

Bates, R L and Jackson, J A (1987). Glossary of geology. Amer. Geol. Inst. Alexandria, Virginia, 788 pp.

Brandl, G (1983). Geology and geochemistry of various supracrustal rocks of the Beit Bridge Complex east of Messina. In : Van Biljon, W J and Legg, J H (Eds). The Limpopo Belt. Spec-Publ. Geol. Soc. S. Afr., 8, 103-112.

Brandt, R T (1973). The origins of jaspilitic iron ores of Australia. Proceedings of the Kiev Symposium, August 1970, Genesis of Precambrian iron and manganese deposits, 59-68.

Collins, R G (1986). The Zandrivierspoort magnetite deposit, Pietersburg district, northern Transvaal. In : Anhaeusser, C R and Maske, S (Eds). Mineral deposits of southern Afria, I, Geol. Soc. S. Afr., 461-467.

Coward, M P (1983). Some thoughts on the tectonics of the Limpopo Belt. In : Van Biljon, W J and Legg, J H (Eds). The Limpopo Belt. Spec-Publ. Geol. Soc. S. Afr., 8, 175-180.

Coward, M P and Fairhead, J D (1980). Gravity and structural evidence for the deep structure of the Limpopo Belt, southern Africa. Tectonophysics, 68, 31-43.

Droop, G T R (1989). Reaction history of garnet - sapphirine granulites and conditions of Archaean high-pressure granulite-facies metamorphism in the Central Limpopo Mobile Belt, Zimbabwe. J Metamorphic Geol., 7, 383-403.

Du Toit, M C, van Reenen, D D and Roering, C (1983). Some aspects of the geology, structure and metamorphism of the Southern Marginal Zone of the Limpopo Metamorphic Complex. In : Van Biljon, W J and Legg, J H (Eds). The Limpopo Belt. Spec-Publ. Geol. Soc. S. Afr., 8, 121-142.

Eminike, E A (1986). Gravity signature of the Limpopo - Kaapvaal fossil plate boundary in southern Africa. Tectonophysics, 128, 127-137.

Frietch, R (1973). Precambrian iron ores of sedimentary origin in Sweden. Proceedings of the Kiev Symposium, August 1970, Genesis of Precambrian iron and manganese deposits, 77-84.

Goryainov, P M (1973). Structural-tectonic environments of iron-ore process in the Baltic shield Precambrian. Proceedings of the Kiev Symposium, August 1970, Genesis of Precambrian iron and manganese deposits, 95-100.

Gross, G A (1973). The depositional environment of principal types of Precambrian iron-formations. Proceedings of the Kiev Symposium, August 1970. Genesis of Precambrian iron and manganese deposits, 15-22.

Gruss, H (1973). Itabirite iron ores of the Liberia and Guyana Shields. Proceedings of the Kiev Symposium, August 1970. Genesis of Precambrian iron and manganese deposits, 335-360.

Harley, S L (1989). The origins of granulites : a metamorphic perspective. Geol. Mag., 126(3), 215-247.

Harris, N B W, Hawkesworth C J, van Calsteren, P and McDermott, F. (1987). Evolution of continental crust in southern Africa. Earth and Planetary Science Letters, 83, 85-93.

Horrocks, P C (1981). Precambrian geology of an area between Messina and Tshipise, Limpopo Mobile Belt [Ph.D thesis] : Johannesburg, University of the Witwatersrand, 205 pp.

Horrocks, P C (1983). The Precambrian geology of an area between Messina and Tshipise, Limpopo Mobile Belt. In : Van Biljon, W J and Legg, J H (Eds). The Limpopo Belt, Spec-Pub. Geol. Soc. S. Afr., 8, 81-88.

Iscor Ltd (1986). Moonlight laegraadse ystererts afsetting Marnitz, Noordwes Transvaal. Internal company report (not published).

Kleywegt, R J (1988). Gravity signature of the Limpopo - Kaapvaal fossil plate boundary in southern Africa: Discussion. Tectonophysics, 145, 349-350.

Krishnan, M S (1973). Occurrence and origin of the iron ores of India. Proceedings of the Kiev Symposium, August 1970, Genesis of Precambrian iron and manganese deposits, 69-76.

Light, M P R (1982). The Limpopo Mobile Belt : A result of continental collision. Tectonics, 1(4), 325-342.

Mackenzie, W S, Donaldson, C H and Guilford, G (1982). Atlas of igneous rocks and their textures. Longman, London, 148 pp.

Mason, R (1973). The Limpopo mobile belt - southern Africa. Phil. Trans. R. Soc. London, A273, 463-485.

McCourt, S (1983). Archaean lithologies of the Koedoesrand area, north-west Transvaal, South Africa. In : Van Biljon, W J and Legg, J H (Eds). The Limpopo Belt. Spec-Publ. Geol. Soc. S. Afr., 8, 113-120.

Pienaar, J C (1985). Die geologie van die Alldays omgewing in Noord Transvaal [M.Sc thesis]: Johannesburg, Rand Afrikaans University, 158 pp.

S A C S (South African Committee for Stratigraphy) (1980). Stratigraphy of South Africa. Part I (Comp. L E Kent). Lithostratigraphy of the Republic of South Africa, South West Africa/Namibia, and the Republics of Bophuthatswana, Transkei and Venda. Handb. Geol. Surv. S. Afr., 8, 690pp.

Sharma, P V (1987). Magnetic method applied to mineral exploration. Ore Geology Reviews, 2, 323-357.

Smit C A (1984). Petrochemistry and tectonic significance of a chromite-bearing ultramafic suite of rocks in the Limpopo Metamorphic Complex, South Africa. Trans. Geol. Soc. S. Afr., 87, 303-314.

Spry, A (1969). Metamorphic textures. Pergamon Press, Toronto, 350pp.

Stanton, R L (1972). Ore Petrology. McGraw-Hill, New York, 713pp.

Stuart, G W and Zengeni T G (1987). Seismic crustal structure of the Limpopo mobile belt, Zimbabwe. Tectonophysics, 144, 323-335.

Tankard, A J, Jackson, M P A, Erickson, K A, Hobday, D K, Hunter, D R and Minter, W E L (1982). Crustal evolution of southern Africa. Springer Verlag, New York, 523pp.

Trendall, A F (1973a). Time-distribution and type-distribution of Precambrian iron-formations in Australia. Proceedings of the Kiev Symposium, August 1970. Genesis of Precambrian iron and manganese deposits, 49-57.

Trendall, A F (1973b). Iron-formations of the Hammersley Group of Western Australia : type examples of varved Precambrian evaporites. Proceedings of the Kiev Symposium, August 1970. Genesis of Precambrian iron and manganese deposits, 257-270.

Van Reenen, D D (1983). Cordieriet + garnet + hypersthene + biotite-bearing assemblages as a function of changing metamorphic conditions in the Southern Marginal Zone of the Limpopo Metamorphic Complex, South Africa. In : Van Biljon, W J and Legg, J H (Eds). The Limpopo Belt. Spec-Publ. Geol. Soc. S. Afr., 8, 143-168.

Van Reenen, D D, Barton, J M, Roering, C, Smith, C A and Van Schalkwyk, J F (1987). Deep crustal response to continental collision : The Limpopo belt of southern Africa. Geology, 15, 11-14.

Van Reenen, D D and Roering, C (Eds.)(1990). The Limpopo Belt: A field workshop on granulites and deep crustal tectonics. Dept of Geology, Rand Afrikaans University, Johannesburg, 289pp.

Visser, H N (1953). The geology of the Koedoesrand area. Explan. Sheet 36, Geol. Surv. S. Afr., 110pp.

Watkeys, M K (1985). The Precambrian geology of the Limpopo belt north and west of Messina [PH.D thesis]: Johannesburg, University of the Witwatersrand, 349pp.

Watkeys, M K, Light, M P R and Broderick, T J (1983). A retrospective view of the Central Zone of the Limpopo Belt, Zimbabwe. In: Van Biljon, W J and Legg, J H (Eds.). The Limpopo Belt. Spec-Publ. Geol. Soc. S. Afr., 8, 65-80.

Windley, B F (1984). The evolving continents. John Wiley and Sons Ltd., 399pp.

Winkler, G F (1975). Petrogenesis of metamorphic rocks. Springer Verlag, New York, 334pp.

Zitzmann, A (Ed.) (1978). The iron ore deposits of Europe and adjacent areas. Vol I and II, Int. Geol. Congress. Bundesanstalt für Geowissenschaften und Rohstoffe, Hannover 418pp + 386pp.

APPENDIX 1: FREQUENCY DISTRIBUTIONS FOR THE DELETERIOUS ELEMENTS K2O, P, AND S IN THE MOONLIGHT ORES

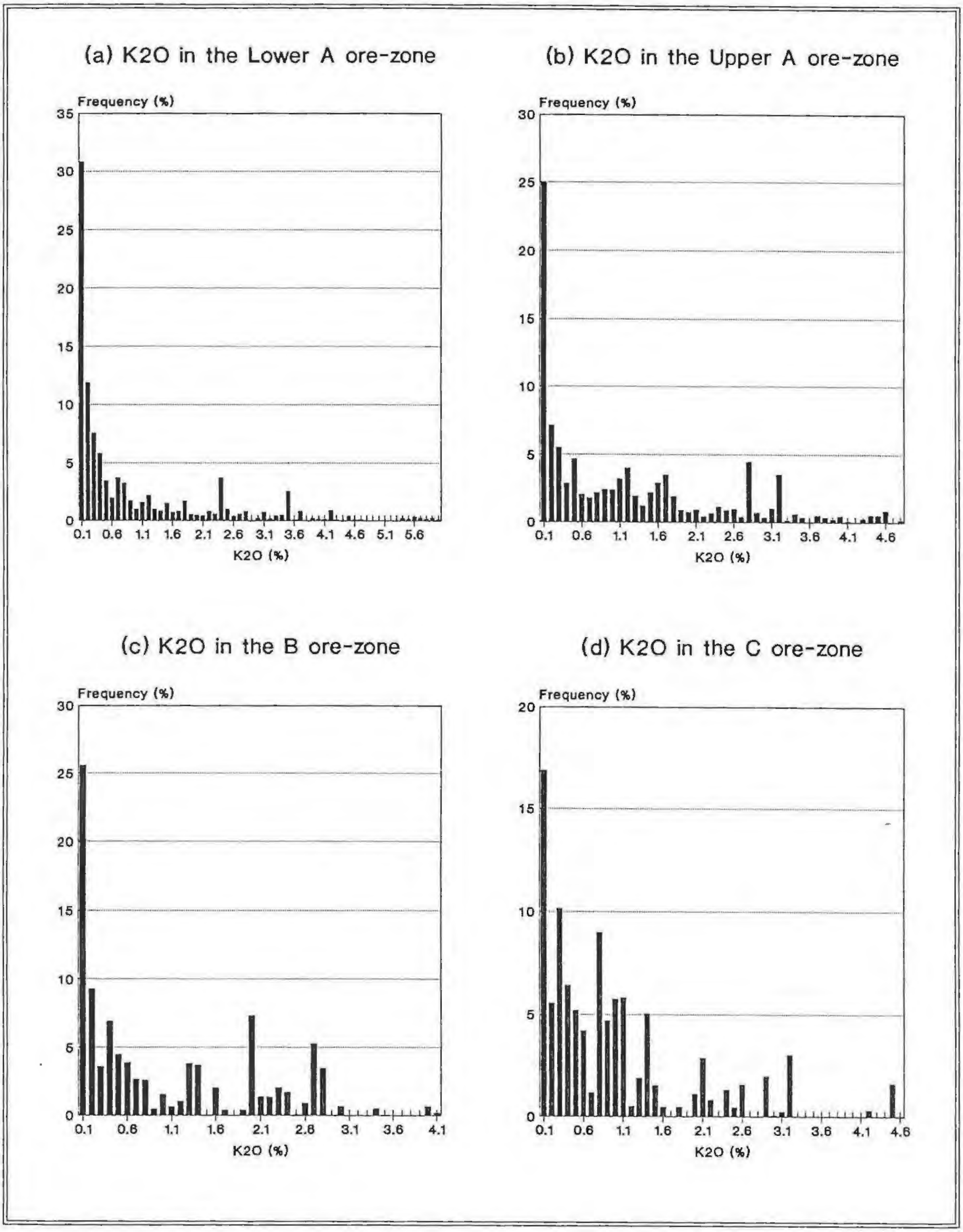

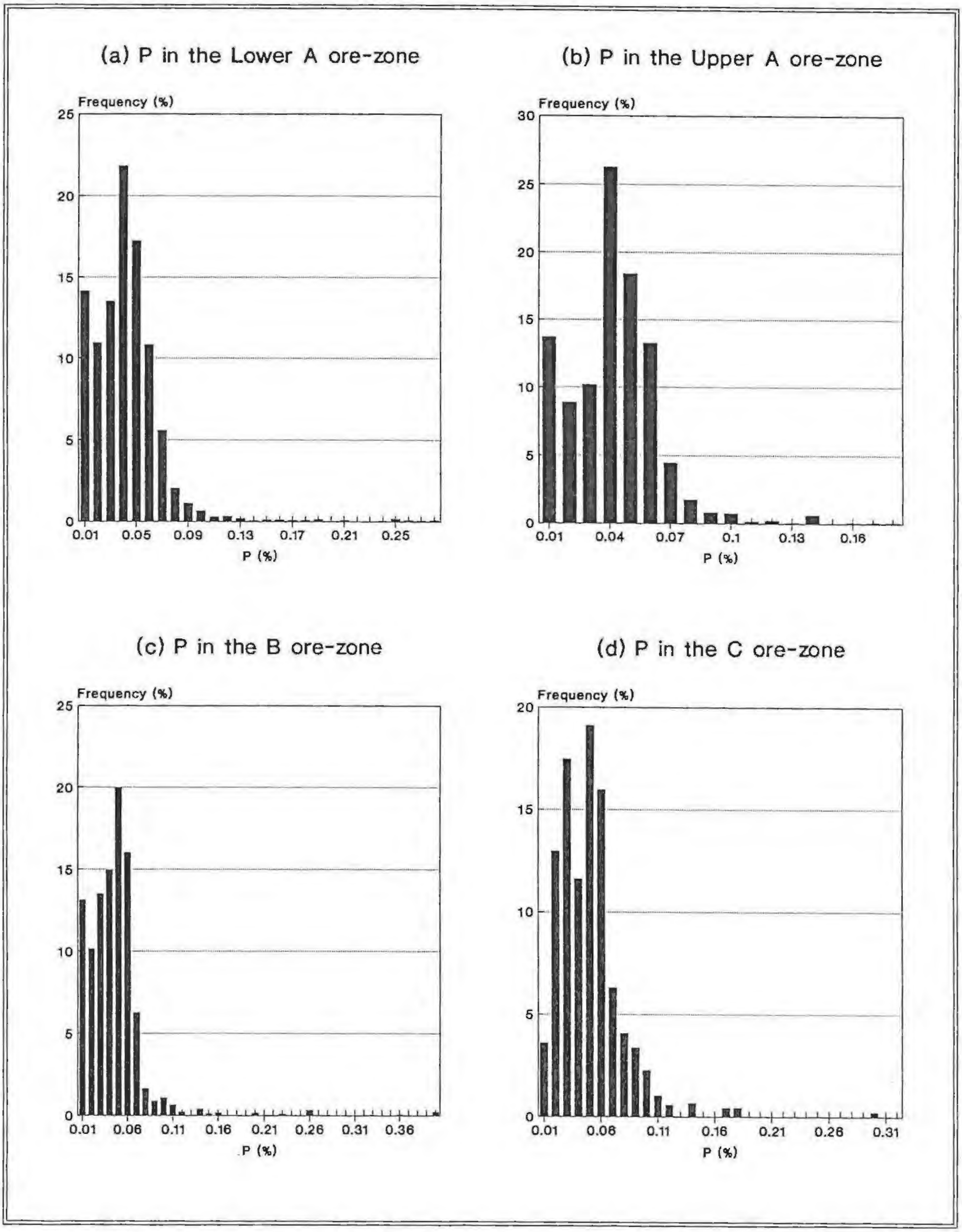
(a) P in the Lower A ore-zone
Frequency (%)
0 5 10 15 20 25
0.01 0.05 0.09 0.13 0.17 0.21 0.25
P (%)
(b) P in the Upper A ore-zone
Frequency (%)
0 5 10 15 20 25 30
0.01 0.04 0.07 0.1 0.13 0.16
P (%)
(c) P in the B ore-zone
Frequency (%)
0 5 10 15 20 25
0.01 0.06 0.11 0.16 0.21 0.26 0.31 0.36
P (%)
(d) P in the C ore-zone
Frequency (%)
0 5 10 15 20
0.01 0.06 0.11 0.16 0.21 0.26 0.31
P (%)

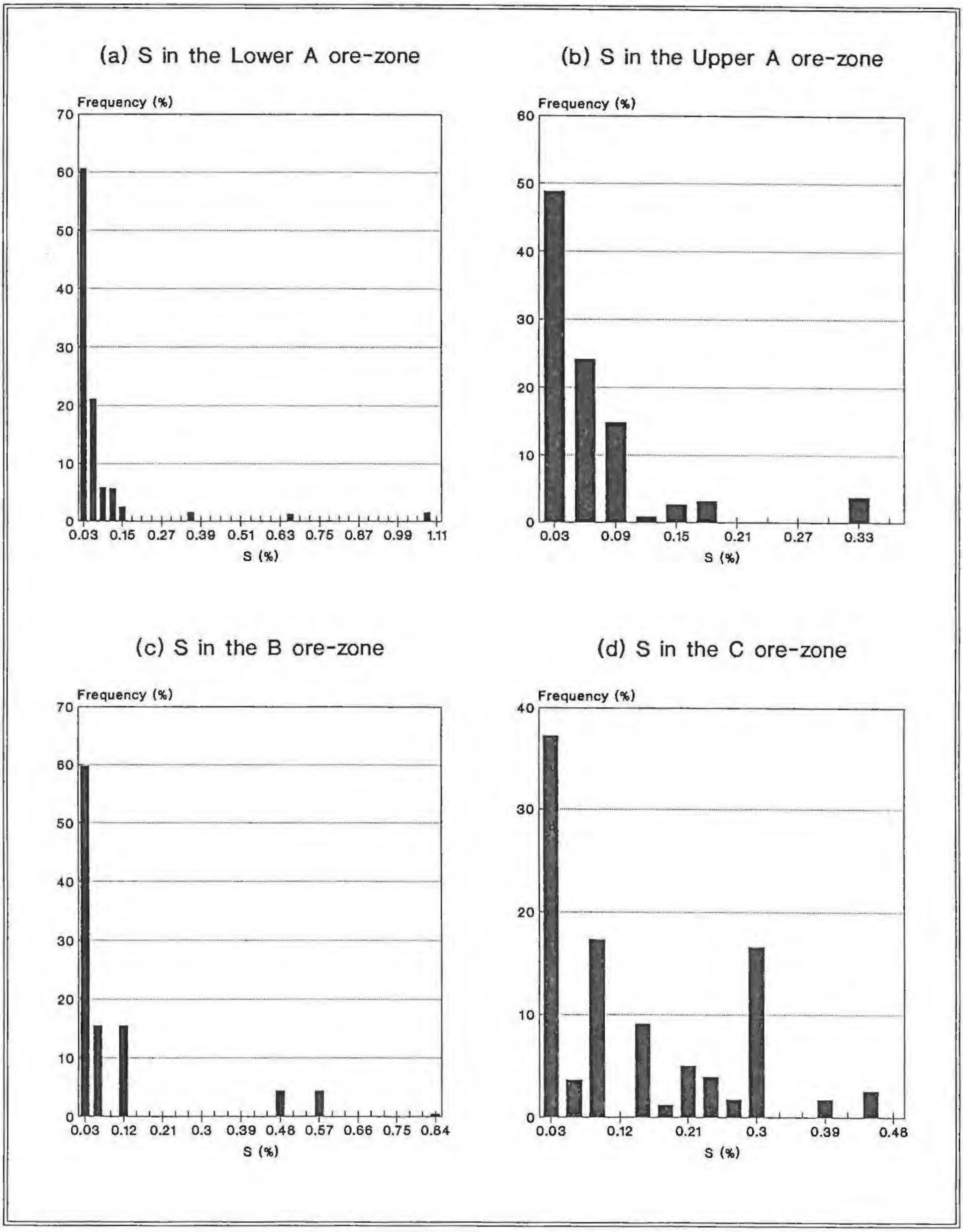
(a) S in the Lower A ore-zone
Frequency (%)
70
60
50
40
30
20
10
0
0.03 0.15 0.27 0.39 0.51 0.63 0.75 0.87 0.99 1.11
S (%)
(b) S in the Upper A ore-zone
Frequency (%)
60
50
40
30
20
10
0
0.03 0.09 0.15 0.21 0.27 0.33
S (%)
(c) S in the B ore-zone
Frequency (%)
70
60
50
40
30
20
10
0
0.03 0.12 0.21 0.3 0.39 0.48 0.57 0.66 0.75 0.84
S (%)
(d) S in the C ore-zone
Frequency (%)
40
30
20
10
0
0.03 0.12 0.21 0.3 0.39 0.48
S (%)

APPENDIX 2: CASH FLOW CALCULATIONS FOR THE MOONLIGHT LOW GRADE IRON ORE DEPOSITS

CASH FLOW FOR THE MOONLIGHT LOW GRADE IRON ORE DEPOSIT
OPTION 1: 180 000 tpm, producing iron ore fines for local consumption

YEARS	0	1	2	3	4	5	6	7	8	9	10
CAPEX	-490										
COSTS		267.48	267.48	267.48	267.48	267.48	267.48	267.48	267.48	267.48	267.48
REVENUE		82.08	82.08	82.08	82.08	82.08	82.08	82.08	82.08	82 08	82.08
CASH FLOW	-490	-185.4	-185.4	-185.4	-185.4	-185.4	-185.4	-185.4	-185.4	-185.4	-185.4
DISCOUNT-factor	1	0.8000	0 6400	0.5120	0.4096	0.3277	0.2621	0.2097	0.1678	0.1342	0.1074
NET PRESENT VALUE	-490	-148.32	-118.656	-94.9248	-75.9398	-60.7518	-48.6014	-38.8811	-31.1049	-24.8839	-19.9071
CUM NPV		-638.32	-756.976	-851.900	-927.840	-988.592	-1037 19	-1076.07	-1107.18	-1132.06	-1151.97

DISCOUNT-factor = 1/(1+i) ^ n , i = discount rate and n = year

Discount rate = 0.25 IRR = -

CASH FLOW FOR THE MOONLIGHT LOW GRADE IRON ORE DEPOSIT
OPTION 2: 160 000 tpm, producing iron ore pellets for local consumption

YEARS	0	1	2	3	4	5	6	7	8	9	10
CAPEX	-730										
COSTS		353.64	353.64	353.64	353.64	353.64	353.64	353.64	353.64	353.64	353.64
REVENUE		259.2	259.2	259.2	259.2	259.2	259.2	259.2	259.2	259.2	259.2
CASH FLOW	-730	-94.44	-94.44	-94.44	-94.44	-94.44	-94.44	-94.44	-94.44	-94 44	-94.44
DISCOUNT-factor	1	0.8	0.64	0.512	0.4096	0.32768	0.262144	0.209715	0.167772	0.134217	0.107374
NET PRESENT VALUE	-730	-75.552	-60.4416	-48.3532	-38.6826	-30.9460	-24.7568	-19.8055	-15.8444	-12.6755	-10.1404
CUM NPV		-805.552	-865.993	-914.346	-953.029	-983.975	-1008.73	-1028.53	-1044.38	-1057.05	-1067.19

DISCOUNT-factor = 1/(1+i) ^ n , i = discount rate and n = year

Discount rate = 0.25 IRR = -

CASH FLOW FOR THE MOONLIGHT LOW GRADE IRON ORE DEPOSIT
OPTION 3: 180 000 tpm, producing iron ore fines FOB Europe

YEARS	0	1	2	3	4	5	6	7	8	9	10
CAPEX	-490										
COSTS		310.32	310.32	310.32	310.32	310.32	310.32	310.32	310.32	310.32	310 32
REVENUE		112.32	112.32	112.32	112.32	112.32	112.32	112.32	112 32	112 32	112 32
CASH FLOW	-490	-198	-198	-198	-198	-198	-198	-198	-198	-198	-198
DISCOUNT-factor	1	0.8	0.64	0.512	0.4096	0.32768	0.262144	0.209715	0.167772	0.134217	0 107374
NET PRESENT VALUE	-490	-158.4	-126.72	-101.376	-81.1008	-64.8806	-51.9045	-41.5236	-33.2188	-26.5751	-21 2600
CUM NPV		-648.4	-775.12	-876.496	-957.596	-1022.47	-1074.38	-1115.90	-1149.12	-1175.69	-1196.95

DISCOUNT-factor = 1/(1+i) ^ n , i = discount rate and n = year

Discount rate = 0 25 IRR =

CASH FLOW FOR THE MOONLIGHT LOW GRADE IRON ORE DEPOSIT
OPTION 4: 180 000 tpm, producing iron ore pellets FOB Europe

YEARS	0	1	2	3	4	5	6	7	8	9	10
CAPEX	-730										
COSTS		397.2	397.2	397.2	397.2	397.2	397 2	397 2	397 2	397 2	397 2
REVENUE		365.04	365.04	365.04	365.04	365.04	365.04	365.04	365.04	365 04	365.04
CASH FLOW	-730	-32.16	-32.16	-32.16	-32.16	-32.16	-32.16	-32 16	-32.16	-32.16	-32.16
DISCOUNT-factor	1	0.8	0.64	0.512	0.4096	0.32768	0.262144	0.209715	0.167772	0.134217	0.107374
NET PRESENT VALUE	-730	-25 728	-20.5824	-16.4659	-13 1727	-10 5381	-8.43055	-6.74444	-5 39555	-4.31644	-3.45315
CUM NPV		-755.728	-776.310	-792.776	-805.949	-816.487	-824.917	-831.662	-837 057	-841.374	-844 827

DISCOUNT-factor = 1/(1+i) ^ n , i = discount rate and n = year

Discount rate = 0.25 IRR = -

CASH FLOW FOR THE MOONLIGHT LOW GRADE IRON ORE DEPOSIT
OPTION 5: 360 000 tpm, producing iron ore fines for local consumption

YEARS	0	1	2	3	4	5	6	7	8	9	10
CAPEX	-595										
COSTS		465.84	465.84	465.84	465.84	465.84	465.84	465.84	465.84	465 84	465 84
REVENUE		164.16	164 16	164.16	164 16	164 16	164.16	164.16	164 16	164 16	164 16
CASH FLOW	-380	-301.68	-301.68	-301.68	-301.68	-301.68	-301 68	-301 68	-301.68	-301 68	-301 68
DISCOUNT-factor	1	0.8	0.64	0.512	0.4096	0.32768	0.262144	0.209715	0.167772	0.134217	0 107374
NET PRESENT VALUE	-380	-241.344	-193.075	-154.460	-123.568	-98.8545	-79.0836	-63 2668	-50.6135	-40.4908	-32.3926
CUM NPV		-621.344	-814.419	-968.879	-1092.44	-1191 30	-1270.38	-1333.65	1384.26	-1424.75	-1457 14

DISCOUNT-factor = 1/(1+i) ^ n , i = discount rate and n = year

Discount rate = 0.25 IRR = -

CASH FLOW FOR THE MOONLIGHT LOW GRADE IRON ORE DEPOSIT
OPTION 6: 360 000 tpm, producing iron ore pellets for local consumption

YEARS	0	1	2	3	4	5	6	7	8	9	10
CAPEX	-921										
COSTS		612.24	812.24	612.24	612.24	612.24	612.24	612.24	612 24	612.24	612 24
REVENUE		518.4	518.4	518.4	518.4	518.4	518.4	518.4	518.4	518.4	518.4
CASH FLOW	-921	-93.84	-93.84	-93.84	-93.84	-93.84	-93.84	-93.84	-93.84	-93.84	-93.84
DISCOUNT-factor	1	0.8	0.64	0.512	0.4096	0.32768	0.262144	0.209715	0.167772	0 134217	0.107374
NET PRESENT VALUE	-921	-75.072	-60.0576	-48.0460	-38 4368	-30.7494	-24.5995	-19.6796	-15.7437	-12.5949	-10.0759
CUM NPV		-996.072	-1056 12	-1104.17	-1142.61	-1173.36	-1197.96	-1217.64	-1233 38	-1245.98	-1256.05

DISCOUNT-factor = 1/(1+i) ^ n , I = discount rate and n = year

Discount rate = 0.25 IRR = -

CASH FLOW FOR THE MOONLIGHT LOW GRADE IRON ORE DEPOSIT
OPTION 7. 360 000 tpm, producing iron ore fines FOB Europe

YEARS	0	1	2	3	4	5	6	7	8	9	10
CAPEX	-595										
COSTS		552.24	552 24	552.24	552 24	552.24	552.24	552.24	552.24	552.24	552 24
REVENUE		224.64	224.64	224.64	224.84	224.64	224.64	224.64	224.64	224.64	224.64
CASH FLOW	-595	-327.6	-327.6	-327.6	-327 6	-327.6	-327 6	-327.6	-327.6	-327 6	-327 6
DISCOUNT-factor	1	0 8	0.64	0.512	0.4096	0 32768	0.262144	0.209715	0.167772	0 134217	0.107374
NET PRESENT VALUE	-595	-262.08	-209.664	-167.731	-134.184	-107.347	-85.8783	-68.7026	-54.9621	-43 9697	-35.1757
CUM NPV		-857.08	-1066.74	-1234.47	-1368 66	-1476.00	-1561.88	-1630.58	-1685 55	-1729.52	-1764.69

DISCOUNT-factor = 1/(1+i) ^ n , i = discount rate and n = year

Discount rate = 0 25 IRR = -

CASH FLOW FOR THE MOONLIGHT LOW GRADE IRON ORE DEPOSIT
OPTION 8: 360 000 tpm, producing iron ore pellets FOB Europe

YEARS	0	1	2	3	4	5	6	7	8	9	10
CAPEX	-921										
COSTS		698.64	698.64	698.64	698.64	698.64	698.64	698.64	698.64	698.64	698 64
REVENUE		730.08	730.08	730.08	730.06	730.08	730.08	730.08	730.08	730.08	730.08
CASH FLOW	-921	31.44	31.44	31.44	31.44	31.44	31 44	31.44	31 44	31.44	31 44
DISCOUNT-factor	1	0.8	0.64	0.512	0.4096	0.32768	0.262144	0.209715	0.167772	0.134217	0 107374
NET PRESENT VALUE	-921	25 152	20.1216	16.09728	12.87782	10.30225	8.241807	6.593445	5.274756	4 219805	3.375844
CUM NPV		-895.848	-875.728	-859.629	-846.751	-836.449	-828.207	-821.613	-816.339	-812 119	-808.743

DISCOUNT-factor = 1/(1+i) ^ n , i = discount rate and n = year

Discount rate = 0.25 IRR = -